Efficient Utility-Preserving Machine Unlearning with Implicit Gradient Surgery

Shiji Zhou[1,2]*†, Tianbai Yu[3], Zhi Zhang[4], Heng Chang[5], Xiao Zhou[5], Dong Wu[6], Han Zhao[3]
[1]Institute of Artificial Intelligence, Beihang University
[2] Beijing Advanced Innovation Center for Future Blockchain and Privacy Computing, Beihang University
[3]University of Illinois at Urbana-Champaign [4]University of Amsterdam
[5]Tsinghua University [6]YanTron Technology Co.Ltd

Abstract

Machine unlearning (MU) aims to efficiently remove sensitive or harmful memory from a pre-trained model. The key challenge is to balance the potential tradeoff between unlearning efficacy and utility preservation, which involves forgetting undesirable information as defined while maintaining the model's original performance. One potential way to tackle this problem is to use multi-objective optimization to jointly optimize both the unlearning and utility preservation objectives. However, existing multi-objective methods only guarantee finding a Pareto-optimal solution without fine-grained control, which causes under-optimization of the unlearning objective. To this end, we first model MU as a constrained optimization problem, that is, optimizing the unlearning objective under the constraint of a bounded increase for utility loss. We then show that solving this optimization problem is equivalent to unilateral gradient surgery on the unlearning objective. To resolve the additional computational cost brought by gradient surgery, we propose an implicit gradient surgery method, which approximates the solution to the aforementioned constrained optimization problem via only one backpropagation, thereby achieving efficient utility-preserving MU. Theoretically, we provide a tight convergence analysis of the algorithm. Empirically, our extensive experiments show that the proposed algorithm achieves better tradeoff results than existing baselines. Codes are available at `https://github.com/anseryuer/EUPMU-Efficient-Utility-Preserving-Machine-Unlearning`.

1 Introduction

The growing capacity of large generative models [39, 5, 74] has inevitably led to increasing concerns about their potential security risks. In particular, massive pre-training data from large models may contain privacy, copyright, and illegal information about individual users, which can be inadvertently memorized through model parameters through training, posing a risk of content leakage under model inversion attacks [21, 71]. Moreover, the high training costs of large models make addressing these issues in pre-trained models particularly challenging [52], since naive retraining is computationally infeasible. Consequently, both industry and academia are actively seeking efficient methods to enable the erasing of sensitive information at a small cost.

Machine unlearning (MU) [4], which aims to enable models to efficiently remove memory of sensitive data, is a potential approach to meet the above goals. The current landscape of MU

[*] Part of the work was done while Shiji Zhou was at Tsinghua University

[†] Corresponding to Shiji Zhou: zhoushiji25@buaa.edu.cn

Shiji Zhou and Tianbai Yu have equal contributions

39th Conference on Neural Information Processing Systems (NeurIPS 2025).

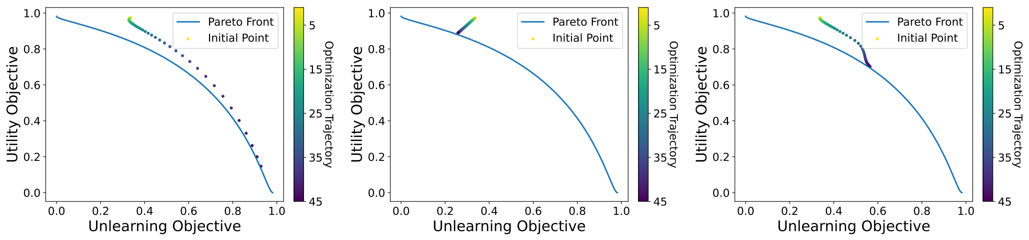

(a) Linear (b) MGDA (c) EUPMU

Figure 1: A showcase where both linear scalarization and MGDA fail to find a good tradeoff solution that balance the utility and unlearning objectives: (a) Linearization often leads to extreme solutions with deterioration on one objective; (b) The pre-trained model fully optimizes the utility objective, leaving little room to improve unlearning objective for MGDA algorithm that fairly optimizes all objectives; (c) Our EUPMU algorithm provides a tolerance for small degradation for utility objective, and returns a better tradeoff solution.

research encompasses a range of generative models, such as large language models (LLM)[68], image synthesis models [50], and multi-modal generative frameworks [59]. These investigations have showcased the capacity of MU to eliminate specific data, including copyrighted patterns [22], fake personas [17], and confidential information [60]. However, the utility-unlearning tradeoff is a key issue in MU [47], where there is a fundamental tradeoff between enhancing the unlearning effect and maintaining the model's original performance. This often leads to a degradation of the model's performance when unlearning sensitive information. Current solutions involve incorporating a retaining loss, calculated from the retained portion of the training data, into the unlearning training process, which can alleviate some of the issues with utility degradation [1, 18]. However, simply combining unlearning and retaining objectives that have inherent conflict fails to find a balanced solution, as it has been proved in multitask learning literature [34], as demonstrated in Figure 1(a).

A potential way to mitigate the conflicts between the two targets is to employ a multi-objective optimization (MOO) [77]. However, existing MOO methods cannot control the converged solutions in a fine-grained way. Specifically, pre-trained models have already been thoroughly optimized for utility, hence it is already or near to a Pareto optimal solution on the Pareto front between unlearning and utility. Since there is little room for further optimization of the utility objectives, directly applying MOO methods that often fairly optimize all objectives to the unlearning problem may result in insufficient optimization of the unlearning objectives, as demonstrated in Figure 1(b). Moreover, most existing MOO methods require derivatives for each objective, doubling the number of backpropagation iterations compared to linear weighting methods, thereby doubling the computational cost. This contradicts the high efficiency and low-cost demand of unlearning.

To tackle the challenges, this paper makes the following principal contributions:

1) To better address the utility-unlearning tradeoff, we first formulate the *Utility-Preserving Unlearning Problem (UPUP)*, where the preservation of utility is formulated as a constraint on the increase in retaining loss at each step, with the goal of maximizing the decrease in unlearning loss under this constraint, thereby optimizing the unlearning objective while preserving utility. Solving UPUP leads to a gradient method equivalent to *Unilateral Gradient Surgery*, which subtracts the components of the unlearning gradient that conflict with the retaining gradient. This ensures that utility degradation is within a controllable range while maxing the erasing of target information.

2) Explicit gradient surgery inevitably doubles the gradient computation. This paper first presents an *Efficient Utility-Preserving Machine Unlearning (EUPMU)* method with *Efficient Implicit Gradient Surgery*, utilizing the essence of gradient surgery being equivalent to dynamic linear weighting. Solving the weights through a first-order approximation, requires only one pass of gradient computation, thus saving up to 50% of the main computational costs. Furthermore, we provide a multi-objective convergence analysis for the proposed algorithm, proving that the algorithm can efficiently converge to a Pareto optimal (or stationary) solution, demonstrating that the algorithm can achieve sufficient unlearning while preserving utility.

3) We conducted comprehensive experiments on tasks including image classification and image generation. Both numerical and visual results demonstrated significant improvements, effectively

proving that our method can fully optimize the unlearning objective while maintaining utility to the greatest extent. This further validates the design and theoretical outcomes of our approach.

2 Background

We begin by introducing the basic concepts of machine unlearning, elucidating the utility-unlearning challenge encountered by existing methods. We then present the concept of Multi-Objective Optimization (MOO) as a potential solution to this problem and discuss why MOO cannot be directly applied to address the challenges in MU. We defer detailed comparison with related works in Appendix A.

2.1 Machine Unlearning

Given the *training dataset* $\mathcal{D} = \{z_i = (x_i, y_i)\}_{i=1}^N$, the original/pre-trained model with parameters $\boldsymbol{\theta}_0$ is encapsulated by the following optimization:

$$\boldsymbol{\theta}_0 = \arg\min_{\theta} \mathbb{E}_{z\sim\mathcal{D}}\ell(z;\boldsymbol{\theta}).$$

MU focuses on eliminating the influence of a specific data subset $\mathcal{D}_f \subset \mathcal{D}$, which is the *forgetting dataset* that may include harmful or sensitive information. The goal is to efficiently derive an unlearned model θ_u by finetuning the original parameters $\boldsymbol{\theta}_0$, while maintaining the model's performance on the *retaining dataset* $\mathcal{D}_r = \mathcal{D} \setminus \mathcal{D}_f$.

To counteract the impact of the forgetting dataset $\mathcal{D}_f$, MU algorithms often establish objectives that aim to reverse the effects of the initial training[3]. These include objectives such as inverse loss [61] and random labeling [24]. We denote this corrective objective as the *unlearning objective* $\ell_u(\boldsymbol{\theta})$. Furthermore, to maintain performance on the remaining data, most MU methods incorporate an objective that mimics retraining on samples from the retaining dataset $\mathcal{D}_r$. This is known as the *retaining objective* $\ell_r(\boldsymbol{\theta})$. Typically, these objectives are linearly combined into one objective [18]:

$$\ell_u(\boldsymbol{\theta}) + \lambda\ell_r(\boldsymbol{\theta}),$$

where λ is a hyperparameter balancing the two parts.

Utility-Unlearning Challenge. While linearization is straightforward to implement, it may lead to performance deterioration or insufficient unlearning, due to the inherent conflict between the unlearning and retaining objectives [72, 75]. The underlying theoretical reason may be that fixed linear weights fails to find a solution that balances the two objectives [34], as shown in Figure 1. (a).

2.2 Multi-Objective Optimization

Multiple-objective optimization (MOO) aims to optimize multiple objectives simultaneously [77]:

$$\min_{\boldsymbol{\theta}} \boldsymbol{L}(\boldsymbol{\theta}) = (\ell^1(\boldsymbol{\theta}), \dots, \ell^m(\boldsymbol{\theta}))^\top, \tag{1}$$

where $m \geq 2$ denotes the number of objectives, and $\ell^i : \mathbb{R}^n \to \mathbb{R}$ is the i-th loss function. Denote Δ_m to be the $(m-1)$-dimensional probability simplex. The concept of Pareto optimality/stationary [12] is introduced to determine whether a solution to MOO is optimal/critical.

Definition 2.1. Pareto Optimality: For any two solutions $\boldsymbol{\theta}, \boldsymbol{\theta}'$, we say that $\boldsymbol{\theta}$ dominates $\boldsymbol{\theta}'$, denoted as $\boldsymbol{\theta} \prec \boldsymbol{\theta}'$ or $\boldsymbol{\theta}' \succ \boldsymbol{\theta}$, if $\ell^i(\boldsymbol{\theta}) \leq \ell^i(\boldsymbol{\theta}')$ for all i, and there exists one i such that $\ell^i(\boldsymbol{\theta}) < \ell^i(\boldsymbol{\theta}')$. A solution $\boldsymbol{\theta}^* \in$ is called Pareto optimal if it is not dominated by any other solution. **Pareto Stationary:** A solution $\boldsymbol{\theta}$ is called Pareto stationary if there exists $\boldsymbol{\lambda} \in \Delta_m$ such that $\sum_{i=1}^m \lambda_i \nabla_{\boldsymbol{\theta}} \ell_i(\boldsymbol{\theta}) = 0$.

Typical MOO methods like MGDA [14], PCGrad [69] and other variants [46, 76, 45, 28] aim to search for a direction $\boldsymbol{d}$ that is not conflicting with each gradient, i.e., $\nabla\ell^i(\boldsymbol{\theta})^\top d \geq 0, i \in [m]$. Using such a non-conflicting direction d_k as the update direction is shown to get better tradeoff performance.

Can MOO Solve Utility-Unlearning Tradeoff? MOO addresses conflicts among objectives during the optimization process and may offer a solution to the utility-unlearning challenge in MU. However,

[3] We here consider approximate unlearning, since exact unlearning often needs to retrain the model, which is impractical for large models due to the high retraining cost.

the optimization goals of MOO and MU are not aligned, making existing MOO methods inadequate for unlearning in pre-trained models. Specifically, pre-trained models have been thoroughly optimized for the utility objective, while the unlearning objective has not been optimized. Therefore, the goal of unlearning is to fully optimize the unlearning objective while maintaining utility to the greatest extent possible, albeit with some minor degradation if necessary, like the solution in Figure 1. (c). However, the primary goal of typical MOO methods is to identify an optimization path that benefits all objectives simultaneously. Given that there is little room for further improvement in utility objectives, directly applying MOO methods to optimize utility and unlearning objectives fairly could lead to inadequate optimization of the unlearning objective, as shown in Figure 1. (b). In addition, MOO often requires gradient computation for each objective, which doubles the computational cost of linearization, which only needs to compute the gradient of the linearized loss.

3 Efficient Utility-Preserving Machine Unlearning

This section first presents the formulation of the Utility-Preserving Unlearning Problem (UPUP). Then, we introduce a gradient method for solving UPUP, which is equivalent to explicit unilateral gradient surgery. To address the additional computational cost brought by gradient surgery, we propose a method of implicit efficient gradient surgery, an efficient approximation for solving UPUP (Algorithm 1). Finally, we provide a theoretical analysis of the Pareto optimality/stationary.

3.1 Utility-Preserving Unlearning Problem

At iteration t, we perform the update $\boldsymbol{\theta}_{t+1} = \boldsymbol{\theta}_t - \alpha_t \boldsymbol{d}_t$ where $\boldsymbol{d}_t$ is the update direction, and define the improvement of the retaining and unlearning objectives as follows

$$r_r(\alpha_t, \boldsymbol{d}_t) = \ell_r(\boldsymbol{\theta}_t) - \ell_r(\boldsymbol{\theta}_{t+1}), r_u(\alpha_t, \boldsymbol{d}_t) = \ell_u(\boldsymbol{\theta}_t) - \ell_u(\boldsymbol{\theta}_{t+1}).$$

To achieve utility-preserving unlearning, we aim to seek a direction $\boldsymbol{d}_t$ to control the degradation of the local retaining target r_r during the constrained optimization process while maximizing the optimization of the unlearning objective. Mathematically, this can be expressed as:

$$\begin{aligned} \max_{\boldsymbol{d}_t} \quad & \frac{1}{\alpha_t} r_u(\alpha_t, \boldsymbol{d}_t) - \frac{1}{2} \left\| \boldsymbol{d}_t \right\|^2 \\ \text{s.t.} \quad & \frac{1}{\alpha_t} r_r(\alpha_t, \boldsymbol{d}_t) \geq -\varepsilon_t, \end{aligned} \tag{2}$$

where α_t is the stepsize, and $\left\| \boldsymbol{d}_t \right\|^2$ is the regularization to avoid unbounded solutions. Here, $\varepsilon_t \geq 0$ is the tolerance of the degradation for the retaining target that we aim to preserve, and the constraint $\frac{1}{\alpha_t} \cdot r_r(\alpha_t, \boldsymbol{d}_t) \geq -\varepsilon_t$ ensures that the utility performance drop is controllable.

3.2 Explicit Unilateral Gradient Surgery

Since stepsize α_t is usually small, by the first-order Taylor approximation, we know that

$$r_r(\alpha_t, \boldsymbol{d}_t) \approx \alpha_t \nabla \ell_r(\boldsymbol{\theta}_t) \cdot \boldsymbol{d}_t, r_u(\alpha_t, \boldsymbol{d}_t) \approx \alpha_t \nabla \ell_u(\boldsymbol{\theta}_t) \cdot \boldsymbol{d}_t.$$

Problem 2 can be approximated by

$$\begin{aligned} \max_{\boldsymbol{d}_t} \quad & \nabla \ell_u(\boldsymbol{\theta}_t) \cdot \boldsymbol{d}_t - \frac{1}{2} \left\| \boldsymbol{d}_t \right\|^2 \\ \text{s.t.} \quad & \nabla \ell_r(\boldsymbol{\theta}_t) \cdot \boldsymbol{d}_t \geq -\varepsilon_t. \end{aligned} \tag{3}$$

Problem 3 aims to control the dot product of $\boldsymbol{d}_t$ and $\nabla \ell_r$ to be greater than $-\varepsilon_t$, thereby ensuring that the degradation of ℓ_r is less than ε_t, while simultaneously maximizing the dot product of $\boldsymbol{d}_t$ and $\nabla \ell_u$ to achieve more effective unlearning.

Proposition 3.1. *The dual objective of Problem 3 is*

$$\min_{\lambda_t \geq 0} L_t(\lambda_t) = \frac{1}{2} \left\| \nabla \ell_u(\boldsymbol{\theta}_t) + \lambda_t \nabla \ell_r(\boldsymbol{\theta}_t) \right\|^2 + \lambda_t \varepsilon_t. \tag{4}$$

Problem 4 has a closed form solution, and the desired direction $\boldsymbol{d}_t^*$ can be solved as

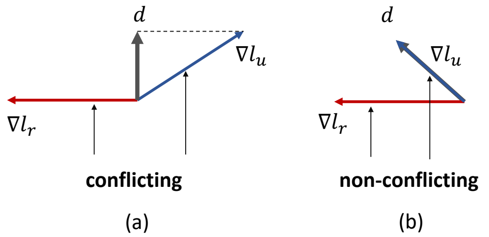

Figure 2: Illustration of Unilateral Gradient Surgery. The computation of the update direction is divided into two scenarios: (a) If the gradient of the unlearning objective conflicts with the gradient of the retaining objective, that is, the angle between them is greater than 90 degrees, the desired direction is obtained by removing the projection (to the retaining gradient) component from the unlearning gradient; (b) If the gradient of the unlearning objective does not conflict with the gradient of the retaining objective, then the unlearning gradient itself is the desired direction.

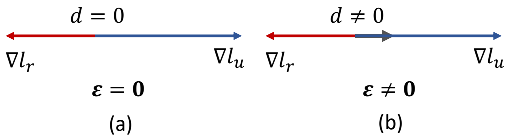

$d = 0$
∇l_r
∇l_u
$\boldsymbol{\varepsilon} = \mathbf{0}$
(a)
$d \neq 0$
∇l_r
∇l_u
$\boldsymbol{\varepsilon} \neq \mathbf{0}$
(b)

Figure 3: Illustration of the role of ε_t. (a) When $\varepsilon_t = 0$, if the retaining gradient and the unlearning gradient are opposite in direction, the update direction $d = 0$, at which point optimization halts and no further progress can be made in optimizing the unlearning objective. (b) When $\varepsilon_t \neq 0$, the update direction $d \neq 0$, and optimization of the unlearning objective proceeds under the condition that it does not unduly affect the retaining objective.

Proposition 3.2. *The closed form solution of Problem 3*

$$\boldsymbol{d}_t^* = \begin{cases} \nabla \ell_u(\boldsymbol{\theta}_t) + \lambda_t^* \nabla \ell_r(\boldsymbol{\theta}_t), & \textit{if } \lambda_t^* > 0 \\ \nabla \ell_u(\boldsymbol{\theta}_t), & \textit{if } \lambda_t^* \leq 0 \end{cases} \tag{5}$$

where

$$\lambda_t^* = \frac{-\nabla \ell_r(\boldsymbol{\theta}_t) \cdot \nabla \ell_u(\boldsymbol{\theta}_t) - \varepsilon_t}{\|\nabla \ell_r(\boldsymbol{\theta}_t)\|^2}. \tag{6}$$

Due to space limit, we defer the derivation details to the Appendix C.2 & C.3. It is worth noting that when $\varepsilon_t = 0$, the direction of $\boldsymbol{d}_t^*$ is equivalent to performing unilateral gradient surgery on the gradient of the unlearning objective, $\nabla \ell_u(\boldsymbol{\theta}_t)$. As illustrated in Figure 2, when $\nabla \ell_u(\boldsymbol{\theta}_t)$ is in conflict with the gradient of the retaining objective, $\nabla \ell_r(\boldsymbol{\theta}_t)$, the direction $\boldsymbol{d}_t^*$ is obtained by eliminating the conflicting component of $\nabla \ell_u(\boldsymbol{\theta}_t)$ along $\nabla \ell_r(\boldsymbol{\theta}_t)$. When $\nabla \ell_u(\boldsymbol{\theta}_t)$ and $\nabla \ell_r(\boldsymbol{\theta}_t)$ are not in conflict, then $\boldsymbol{d}_t^* = \nabla \ell_u(\boldsymbol{\theta}_t)$, and directly optimizing the unlearning objective will not have a negative impact on the retaining objective.

When $\varepsilon_t \neq 0$, an error tolerance is introduced, gradient surgery is only performed when the conflict between the unlearning and the retaining gradients is sufficiently large, that is, when $\nabla \ell_r(\boldsymbol{\theta}_t) \cdot \nabla \ell_u(\boldsymbol{\theta}_t) < -\varepsilon_t$. This threshold controls the priority during the optimization process for the unlearning objective. Specifically, when the angle between the retaining gradient and the unlearning gradient is 180 degrees as illustrated in Figure 3, if $\varepsilon_t = 0$, the optimization process stops and the unlearning objective can not be further optimized. In contrast, when $\varepsilon_t \neq 0$, a certain degree of optimization for the unlearning objective is still guaranteed.

Remark 3.3. We can demonstrate that by imposing local constraints on the retaining objective at each training step, the decline in utility throughout the entire optimization process can be controlled by

$$\ell_r(\boldsymbol{\theta}_t) - \ell_r(\boldsymbol{\theta}_0) \lesssim \mathcal{O}\left(\sum_{i=1}^{t} \varepsilon_t \alpha_t\right). \tag{7}$$

Proof details are deferred to the Appendix C.4. This illustrates that the increase in the retaining objective is controlled by $\sum_{i=1}^{t} \varepsilon_t \alpha_t$. This indicates that we can achieve the goal of utility-preservation by adjusting the hyperparameters.

3.3 Implicit Efficient Gradient Surgery

Although unilateral gradient surgery can ensure that the optimization results meet the expected utility-preserving criteria, the computational cost in the optimization process is double that of the linear weighting method due to the need to calculate gradients for both the unlearning and retaining objectives separately. This can lead to inefficiency in optimization, which contradicts the high-efficiency and low-cost goals that unlearning aims to achieve. To tackle this challenge, we propose an efficient approximate solution to Problem 3 in the following section, which requires only a single step of backpropagation, making the computational cost equivalent to that of the linear weighting method.

Since the solution to Problem 4 requires knowledge of the gradients for both the unlearning and retaining objectives, we consider using a gradient descent approximation to solve for λ_t:

$$\lambda_{t+1} = \lambda_t - \beta_t \nabla_{\lambda_t} L_t(\lambda_t).$$

However, the gradient of $L_t(\lambda_t)$ still necessitates information about the gradients of the unlearning and retaining objectives. Therefore, we consider approximating the gradient $\nabla_{\lambda_t} L_t(\lambda_t)$ using first-order Taylor's approximation:

$$\begin{aligned} \nabla_{\lambda_t} L_t(\lambda_t) &= \nabla \ell_r(\boldsymbol{\theta}_t) \cdot (\nabla \ell_u(\boldsymbol{\theta}_t) + \lambda_t \nabla \ell_r(\boldsymbol{\theta}_t)) + \varepsilon_t \\ &= \nabla \ell_r(\boldsymbol{\theta}_t) \cdot \boldsymbol{d}_t + \varepsilon_t \\ &\approx \frac{1}{\alpha_t}(\ell_r(\boldsymbol{\theta}_t) - \ell_r(\boldsymbol{\theta}_{t+1})) + \varepsilon_t. \end{aligned}$$

Consequently, we have an approximate method for solving λ_t without backpropagation:

$$\begin{aligned} \lambda_{t+1} &= \lambda_t - \beta_t \tilde{\delta}_t, \\ \text{where } \tilde{\delta}_t &= \frac{1}{\alpha_t}(\ell_r(\boldsymbol{\theta}_t) - \ell_r(\boldsymbol{\theta}_{t+1})) + \varepsilon_t. \end{aligned} \tag{8}$$

We provide the complete Efficient Utility-Preserving Machine Unlearning (EUPMU) algorithm (Algorithm 1) in Appendix B. The algorithm first computes the approximated weight λ_t by Eq.8 with no backpropagation of the loss function, and then uses λ_t to compute the update direction d_k by one backpropagation of the composite loss $\ell_u(\boldsymbol{\theta}_t) + \lambda_t \ell_r(\boldsymbol{\theta}_t)$. Finally, the model parameter is updated by one gradient step with d_k. This process does not require to compute $\nabla \ell_u(\boldsymbol{\theta}_t)$ and $\nabla \ell_r(\boldsymbol{\theta}_t)$ separately like traditional multi-objective method, and hence save half of the computational cost.

A faster version of EUPMU. We propose EUPMU-fast as a lightweight variant of EUPMU that removes the second retain-loss recomputation on the same batch. Concretely, whereas EUPMU estimates the retain-loss change at step t as $\Delta_r^{(t)} = \ell_r(\theta_t; \mathcal{B}_r^{(t)}) - \ell_r(\theta_{t+1}; \mathcal{B}_r^{(t)})$, which requires an extra forward pass at θ_{t+1} on $\mathcal{B}_r^{(t)}$, EUPMU-fast uses a stochastic proxy based on consecutive retain batches:

$$\widehat{\Delta}_r^{(t)} \;\approx\; \ell_r(\theta_{t+1}; \mathcal{B}_r^{(t+1)}) \;-\; \ell_r(\theta_t; \mathcal{B}_r^{(t)}),$$

so it incurs no additional forward pass. This reduces wall-clock per step (see RTE) but can be less stable due to between-batch variation; in our runs, it sometimes underperforms EUPMU, though it remains competitive while being slightly faster.

3.4 Theoretical Analysis

Our primary concern is whether λ_t in Algorithm 1 can approximate the property of the optimal solution λ_t^*, which determines whether efficient gradient surgery can achieve the goal of utility-preservation. Therefore, we present the following theorem to elucidate this result.

Theorem 3.4 (Approximate λ^*). *Suppose retaining objective and unlearning objective are both (i) G-Smooth; (ii) L-Lipschitz. At training step t, setting* $\sum_{i=0}^{t} \alpha_i \leq \mathcal{O}(1)$, $\beta_i/\alpha_i = \mathcal{O}(1/t^{1/3})$ *and* $\sum_{i=0}^{t} \varepsilon_i \leq \mathcal{O}(1)$, *we have*

$$\frac{1}{t}\sum_{i=1}^{t} (L_i(\lambda_i) - L_i(\lambda_i^*)) \leq \mathcal{O}(1/t^{1/3}) \tag{9}$$

Table 1: Performance of class-wise forgetting on Imagenette using SD. The best performance is highlighted in **bold**.

Forget.Class	SalUn		ESD		FMN		EUPMU	
	UA	FID	UA	FID	UA	FID	UA	FID
Tench	0.00	0.94	0.00	1.18	56.20	**0.86**	0.00	0.93
EnglishSpringer	0.00	**0.79**	0.00	0.98	71.40	1.24	0.00	1.52
CassettePlayer	0.20	1.59	3.40	1.75	11.20	1.02	0.00	**0.97**
ChainSaw	0.00	1.07	0.00	1.55	50.80	**0.88**	0.00	0.99
Church	0.40	0.99	2.60	1.88	75.60	1.66	0.00	**0.87**
FrenchHorn	0.00	1.44	0.40	1.15	54.40	1.88	0.00	**0.83**
GarbageTruck	0.00	1.63	0.20	2.38	58.00	1.10	0.00	**1.06**
GasPump	0.00	**0.81**	1.00	2.03	23.60	1.36	0.00	1.04
GolfBall	1.20	1.89	3.20	**0.85**	83.80	1.12	0.00	1.28
Parachute	0.00	1.06	0.00	1.54	64.80	2.22	0.00	**0.79**
Average	0.18	1.22	1.09	1.46	59.76	1.27	**0.00**	**1.03**

Theorem 3.4 demonstrates that as the training step increases, $L_t(\lambda_t)$ gradually converges to $L_t(\lambda_t^*)$, indicating that when t is sufficiently large, λ_t can approximate the condition for utility-preservation.

We next focus on whether Algorithm 1 can converge to a Pareto optimal solution, which would indicate whether the algorithm can fully optimize the unlearning objective under utility-preservation.

Theorem 3.5 (Pareto Optimality)**.** *Suppose retaining objective and unlearning objective are both (i) convex with parameter $\boldsymbol{\theta}$; (ii) bounded by B; (iii) L-Lipschitz; (iv) $\|\boldsymbol{\theta}_t\|$ is bounded by B for $t = 1, \ldots, T$. At training step t, setting $\alpha_i = \alpha \leq \mathcal{O}(1/G)$, $\sum_{i=0}^{t}(i+1)\beta_i \leq \mathcal{O}(1)$, and $\sum_{i=0}^{t} \varepsilon_i \leq \mathcal{O}(1)$, there exist composite loss $\mathcal{C}(\boldsymbol{\theta}) = \mu_u \ell_u(\boldsymbol{\theta}) + \mu_r \ell_r(\boldsymbol{\theta})$, $(\mu_u, \mu_r) \in \Delta_2$ such that*

$$\mathcal{C}(\boldsymbol{\theta}_t) - \min_{\boldsymbol{\theta}} \mathcal{C}(\boldsymbol{\theta}) \leq \mathcal{O}(1/t). \tag{10}$$

Theorem 3.5 establishes the convergence in the convex case, confirming that Algorithm 1 converges to a Pareto optimal solution, and the convergence order matches that of the current state-of-the-art first-order MOO algorithms.

Remark 3.6. More specifically, combining Equation 7 and Theorem 3.5, we can bound the optimality of the unlearning objective by $\ell_u(\boldsymbol{\theta}) - \ell_u(\boldsymbol{\theta}^*) \leq \mathcal{O}(1/t)$, where $\boldsymbol{\theta}^* = \max_{\boldsymbol{\theta}} \ell_u(\boldsymbol{\theta})$, s.t. $\ell_r(\boldsymbol{\theta}) - \ell_r(\boldsymbol{\theta}_0) \lesssim \mathcal{O}\left(\sum_{i=1}^{t} \varepsilon_t \alpha_t\right)$. It shows that EUPMU converges to the solution with optimal unlearning objective under the constraint of a slight deterioration for retaining objective. This demonstrates that the unlearning objective is sufficiently optimized.

Theorem 3.7 (Pareto Stationary)**.** *Suppose retaining objective and unlearning objective are both (i) G-Smooth; (ii) bounded by B; (iii) L-Lipschitz. At training step t, setting $\alpha_i = \alpha \leq \mathcal{O}(1/G)$, $\sum_{i=0}^{t}(i+1)\beta_i \leq \mathcal{O}(1)$, and $\sum_{i=1}^{t} \varepsilon_i \leq \mathcal{O}(1)$, we have*

$$\min_{i=1,\ldots,t} \min_{(\mu_u,\mu_r)\in\Delta_2} \|\mu_u \nabla \ell_u(\boldsymbol{\theta}_i) + \mu_r \nabla \ell_r(\boldsymbol{\theta}_i)\| \leq \mathcal{O}(1/t^{1/2}) \tag{11}$$

Theorem 3.7 elucidates the convergence in the non-convex scenario, demonstrating that Algorithm 1 is capable of converging to a Pareto stationary point, with a convergence order that remains on par with the current best first-order multi-objective optimization algorithms. This indicates that the algorithm theoretically ensures sufficient and efficient optimization even in non-convex situations. We defer all the proof details to the Appendix C.5, C.6, C.7, C.8.

4 Experiments

In this section, we present empirical assessments of our proposed approach through experiments on image generation tasks, and benchmark its performance against a number of contemporary MU baselines. We leave detailed setups and results as well as additional experiments in Appendix D

Table 2: Quantitative results of instance unlearning and artist style unlearning. The best-performing results are highlighted in **bold**, and the second-best results are underlined.

Model	**Snoopy**			**Mickey**			**Spongebob**			**Van Gogh**			**Picasso**			**Rembrandt**		
	CS	CA	FID	CS	CA	FID	CS	CA	FID	CS	CA	FID	CS	CA	FID	CS	CA	FID
SD v1.4	74.48	99.38	-	72.43	97.62	-	73.06	98.50	-	73.20	94.75	-	69.01	90.74	-	71.65	95.73	-
	Erasing **Snoopy**									Erasing **Van Gogh**								
	CS ↓	CA ↓	FID ↑	CS ↑	CA ↑	FID ↓	CS ↑	CA ↑	FID ↓	CS ↓	CA ↓	FID ↑	CS ↑	CA ↑	FID ↓	CS ↑	CA ↑	FID ↓
ESD	49.27	35.38	139.47	58.48	65.00	112.96	62.06	82.25	103.04	51.85	39.25	179.17	63.79	76.60	79.61	65.49	78.94	91.83
ConAbl	57.32	80.88	139.31	69.43	94.38	56.22	70.60	97.00	61.56	57.40	34.00	167.07	65.65	80.83	57.85	68.66	91.95	78.38
SPM	54.82	75.38	111.42	71.89	**97.5**	30.16	**72.79**	98.12	42.1	51.7	**32.25**	198.43	68.47	89.58	23.64	70.83	94.22	41.51
EUPMU	**44.9**	**25.62**	**167.66**	**72.74**	**97.5**	**29.2**	72.52	**98.88**	**40.2**	**45.01**	33.0	**228.75**	**68.69**	**89.59**	**22.96**	**71.01**	**95.97**	**39.98**
	Erasing **Snoopy and Mickey**									Erasing **Picasso**								
	CS ↓	CA ↓	FID ↑	CS ↓	CA ↓	FID ↑	CS ↑	CA ↑	FID ↓	CS ↑	CA ↑	FID ↓	CS ↓	CA ↓	FID ↑	CS ↑	CA ↑	FID ↓
ESD	48.99	**34.88**	143.29	47.79	23.75	167.05	58.03	68.88	123.11	70.43	86.25	104.56	60.60	51.72	180.50	70.61	93.13	91.70
ConAbl	60.85	94.50	119.62	63.46	87.12	105.99	70.06	97.38	66.82	68.05	83.75	106.20	58.92	51.21	145.65	70.76	94.88	69.09
SPM	54.18	73.00	113.74	53.58	64.38	132.08	**72.37**	97.88	45.44	**73.27**	**94.75**	24.45	48.89	51.24	258.91	71.5	**96.88**	**25.12**
EUPMU	**46.85**	43.25	**161.11**	**44.55**	**21.0**	**196.59**	71.3	**98.63**	**44.84**	73.24	**94.75**	**23.41**	**45.42**	**40.49**	**273.38**	**71.54**	96.37	26.98
	Erasing **Snoopy, Mickey and Spongebob**									Erasing **Rembrandt**								
	CS ↓	CA ↓	FID ↑	CS ↓	CA ↓	FID ↑	CS ↓	CA ↓	FID ↑	CS ↑	CA ↑	FID ↓	CS ↑	CA ↑	FID ↓	CS ↓	CA ↓	FID ↑
ESD	48.6	**34.88**	147.39	46.91	20.12	173.96	45.22	11.38	192.87	66.68	73.00	87.30	68.97	88.18	79.11	41.31	5.97	206.59
ConAbl	60.48	95.62	125.54	61.30	80.75	112.43	60.36	89.38	125.04	67.73	78.25	84.77	67.83	85.20	46.52	55.82	39.46	130.92
SPM	54.17	74.25	114.69	53.76	64.25	131.28	52.15	63.88	154.65	72.81	93.75	30.06	68.83	88.73	17.8	32.23	**0.22**	269.27
EUPMU	**47.01**	43.5	**155.63**	**44.24**	**18.75**	**200.24**	**42.01**	**5.37**	**213.23**	**73.01**	**94.5**	**26.12**	**69.12**	**90.49**	**14.99**	**27.59**	0.48	**274.82**

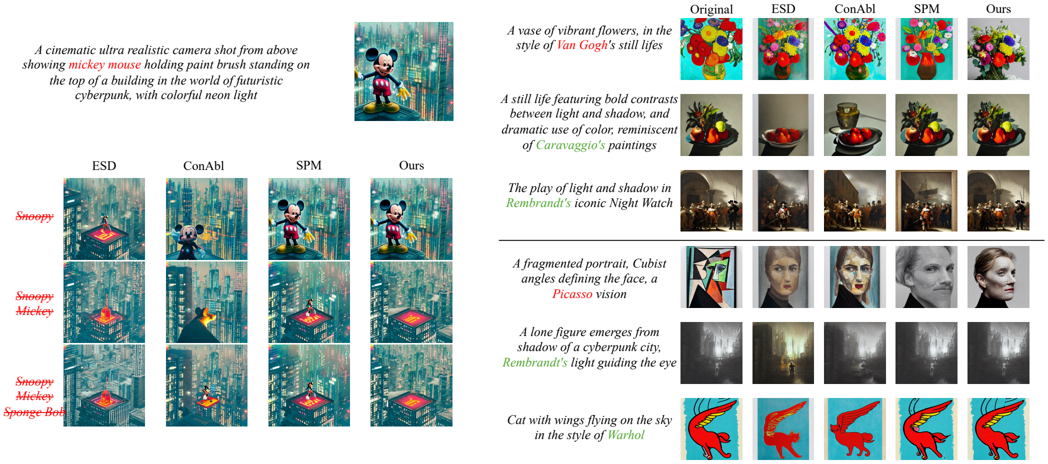
A cinematic ultra realistic camera shot from above showing mickey mouse holding paint brush standing on the top of a building in the world of futuristic cyberpunk, with colorful neon light
ESD
ConAbl
SPM
Ours
~~Snoopy~~
~~Snoopy~~
~~Mickey~~
~~Snoopy~~
~~Mickey~~
~~Sponge Bob~~
Original
ESD
ConAbl
SPM
Ours
A vase of vibrant flowers, in the style of Van Gogh's still lifes
A still life featuring bold contrasts between light and shadow, and dramatic use of color, reminiscent of Caravaggio's paintings
The play of light and shadow in Rembrandt's iconic Night Watch
A fragmented portrait, Cubist angles defining the face, a Picasso vision
A lone figure emerges from shadow of a cyberpunk city, Rembrandt's light guiding the eye
Cat with wings flying on the sky in the style of Warhol

Figure 4: Visualization of instance & style unlearning. Concepts that have been unlearned are indicated in red.

4.1 Experiment Setups

Implementation Details. We focus on DDPM [31] and SD [55] models to prevent the generation of specific object classes, and the experiments are conducted on CIFAR-10 and Imagenette [33], respectively. We also consider concept-wise forgetting in SD to erase instance & style concepts and NSFW (not safe for work) content. All numerical results are the mean value over 5 independent trials. All experiments are carried out on two A100 GPUs.

Baselines. Our experiments encompas baselines, including saliency unlearning (SalUn) [18], erased stable diffusion (ESD) [22], forget-me-not (FMN) [70] and concept ablation (ConAbl) [41].

Evaluation Metrics. Unlearning Accuracy (UA), CLIP Score (CS) [29], CLIP Accuracy [41] (CA), FID [30] and Runtime Efficiency (RTE) are utilized to measure the unlearning performance in concept-wise forgetting tasks. UA employs an external classifier, which is finetuned to classify the Cifar-10 dataset, to confirm the absence of the forgetting concept in generated images. The CLIP Score calculates the similarity between the image and the prompt. CLIP Accuracy is determined by performing a binary classification to distinguish between the target and the anchor concepts. RTE is the relative estimated computation time of applying an MU method.

Table 3: NSFW Content Removal Statistics. We follow the i2p prompts [56] set that contains 4709 samples, and present the number of NSFW contents generated by models before and after unlearning. The unlearning methods include ESD, FMN, SalUn and ours. The best performance is highlighted in **bold**.

Category	SD	FMN	ESD	SalUn	Ours
Male genitalia	54	11	17	3	**0**
Male breast	244	51	39	4	**1**
Female genitalia	28	10	10	2	**0**
Female breast	225	43	30	4	**3**
Buttocks	57	14	12	**0**	2
Total	608	129	108	13	**6**

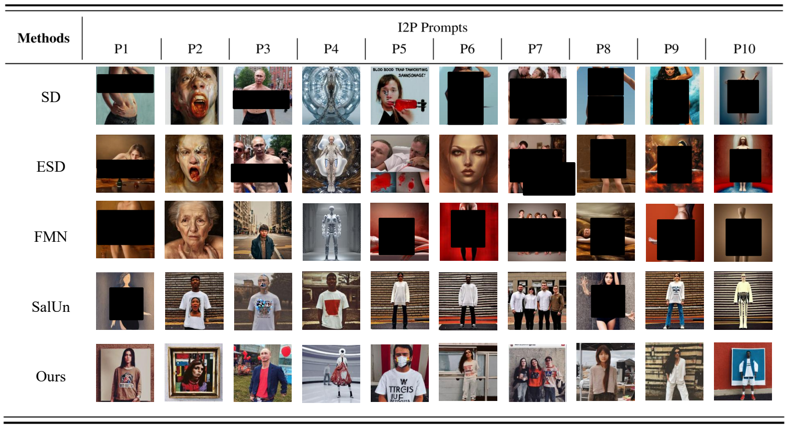

Figure 5: Examples of generated images using SDs w/ and w/o MU. Each column represents generated images with the same prompt (denoted by P_i) and seed.

4.2 Experiment Results

Class-wise Forgetting in Image Generation.

Table 5 presents the numerical results for the unlearning of the category 'Airplane' in DDPM. In the numerical results, our approach shows a significantly better FID score compared to ESD and SalUn, while the UA score is consistent with other methods, demonstrating the utility preservation efficacy of EUPMU, which achieves a superior tradeoff in this task. Table 1 also displays numerical outcomes for SD unlearning across different categories, where EUPMU demonstrates notable improvements in both UA and FID metrics, further confirming the capability of the proposed method to address the utility-unlearning tradeoff issue.

Table 5: Performance of class-wise forgetting on CIFAR-10 with classifier-free guidance DDPM. The best performance is in **bold**.

Method	UA	FID	RTE
Retrain	1.80	20.50	-
ESD	**0.00**	47.57	1.6
SalUn	0.74	24.53	6.05
EUPMU	0.78	**22.57**	**1.38**

Instance & Style Forgetting in Image Generation. We selected several representative concepts to verify the performance of unlearning instances and styles, as detailed in Table 2. In both instance and style forgetting tasks, our approach nearly outperforms other baselines in all metrics of CS, CA and FID, demonstrating that it successfully unlearns specific instances and styles while excelling in preserving non-target concepts. Visualization is shown in Figure 4, we observe that EUPMU can precisely erase target concepts without negative impact on model capability. See Appx. Figure 6 for a 3D Pareto analysis over {CS-Forget, CA-Forget, FID-Retain}, where integrating EUPMU into both ConAbl and SPM significantly improve the Pareto front to all baselines.

NSFW Forgetting in Image Generation. Table 3 and Figure 5 demonstrate the effect of using Machine Unlearning (MU) to forget the illicit concept of nudity. From Table 3, we observe that our method generates the least number of NSFW images, proving that EUPMU more effectively erases NSFW content than other baselines. From Figure 5, we find that the quality of the generated images

Table 4: Ablation of MOO Methods applied to Random Labeling for Class-wise Data Forgetting(10%) of unlearning Resnet 18 for Cifar 10 classification. The best performance is highlighted in **bold**. We define the average score (Avg.score) to be (UA+RA+TA+MIA)/4.

Methods	Description	UA	RA	TA	MIA	Avg. score	RTE
Retrain	Full Retraining	100.00	100.00	94.68	100.00	98.67	-
Linearization	Pure Linearization	98.44	96.88	90.97	100.00	96.57	**15.7**
FAMO	Efficient MGDA	98.68	98.44	92.56	100.00	97.48	**18.7**
PCGrad	Confined Gradient Surgery	98.71	98.64	92.65	100.00	97.50	27.7
UNGrad	Unilateral Gradient Surgery	99.53	99.25	93.70	100.00	98.12	27.7
EUPMU	Efficient Unilateral Gradient Surgery	**99.64**	99.69	94.29	100.00	**98.40**	**18.4**
EUPMU-fast	Fast EUPMU variant	98.18	**99.83**	**94.36**	100.00	98.09	**17.9**

is significantly superior to other methods. This indicates that our approach can effectively achieve concept unlearning without compromising the model's generative capabilities.

4.3 Ablation Study

Table 4 presents the results of our ablation study. We use Unlearning Accuracy (UA) and Membership Inference Attack (MIA) for unlearning efficacy, Remaining Accuracy (RA) and Testing Accuracy (TA) for classifier fidelity. We compared representative MOO methods, FAMO [45] and PCGrad [69]. FAMO is an efficient approximation of the MGDA algorithm, while PCGrad represents the gradient surgery approach. This comparison aims to demonstrate that pure MOO algorithms cannot resolve the utility-unlearning challenge mentioned in the background. Additionally, we contrasted our results with UNGrad, the explicit unilateral gradient surgery method introduced in previous section, to assess whether the implicit efficient gradient surgery in EUPMU can achieve the effectiveness of the exact method and enhance algorithmic efficiency.

MOO can not solve utility-unlearning tradeoff. Comparing RL with RL+FAMO and RL+PCGrad, we observe a consistent improvement across all metrics after employing MOO methods. However, the optimization for UA is not as pronounced. This is attributed to the MOO methods' insufficient optimization of the unlearning goal. Comparing RL+UNGrad with RL+EUPMU, we find that compared to MOO methods, there is sufficient optimization in MIA, indicating that the UPUP modeling approach is better suited for unlearning problems.

Implicit gradient surgery is efficient. Comparing RL+EUPMU with RL+UNGrad and RL+PCGrad, we find a significant reduction in Runtime Efficiency (RTE) of EUPMU, demontrating the efficiency. At the same time, since it only requires one backward pass, RTE is essentially consistent with the linear weighting method. EUPMU-fast further decreases RTE with removing the extra retain loss forward pass and uses next batch retain loss to measure change of retain loss. However the result might be not as good as EUPMU's result, due to the randomness and difference between batches.

Implicit gradient surgery may be more effective than explicit gradient surgery. Comparing RL+EUPMU with RL+UNGrad, we observe a significant improvement in every metric. This is attributed to the fact that under the stochastic gradient training in deep learning, the method of approximating solutions for composite weights λ is more stable than the precise solution, thereby achieving better results [76].

5 Conclusion

This paper investigates the core issue of the utility-unlearning tradeoff in machine unlearning, highlighting that existing multi-objective methods cannot be directly applied to unlearning scenarios due to inconsistencies in modeling with unlearning goals and issues with algorithmic efficiency. Therefore, this paper first establishes the utility-preserving unlearning problem and proposes a gradient-based optimization algorithm to solve it, proving its equivalence to unilateral gradient surgery. Subsequently, an efficient implicit gradient surgery method is introduced to accelerate the efficiency of gradient surgery and avoid introducing additional computational costs. Theoretically, we analyze that the algorithm can converge to Pareto optimal/stationary while maintaining utility, indicating that the algorithm can achieve an optimal tradeoff. Empirically, experimental results validate that the algorithm can fulfill the purpose of utility preservation while sufficiently optimizing the unlearning effect, further corroborating the theoretical findings.

Acknowledgments and Disclosure of Funding

This work is supported by the National Science Foundation of China (62401327). We would like to thank Yongliang Wu for his advice on the experiments.

References

[1] Seohui Bae, Seoyoon Kim, Hyemin Jung, and Woohyung Lim. Gradient surgery for one-shot unlearning on generative model, 2023.

[2] Romain Beaumont. Clip retrieval: Easily compute clip embeddings and build a clip retrieval system with them. `https://github.com/rom1504/clip-retrieval`, 2022.

[3] Alexander Becker and Thomas Liebig. Evaluating machine unlearning via epistemic uncertainty. *arXiv preprint arXiv:2208.10836*, 2022.

[4] Lucas Bourtoule, Varun Chandrasekaran, Christopher A Choquette-Choo, Hengrui Jia, Adelin Travers, Baiwu Zhang, David Lie, and Nicolas Papernot. Machine unlearning. In *2021 IEEE Symposium on Security and Privacy (SP)*, pages 141–159. IEEE, 2021.

[5] Yupeng Chang, Xu Wang, Jindong Wang, Yuan Wu, Linyi Yang, Kaijie Zhu, Hao Chen, Xiaoyuan Yi, Cunxiang Wang, Yidong Wang, et al. A survey on evaluation of large language models. *ACM Transactions on Intelligent Systems and Technology*, 2023.

[6] Min Chen, Weizhuo Gao, Gaoyang Liu, Kai Peng, and Chen Wang. Boundary unlearning: Rapid forgetting of deep networks via shifting the decision boundary. In *Proceedings of the IEEE/CVF Conference on Computer Vision and Pattern Recognition*, pages 7766–7775, 2023.

[7] Min Chen, Zhikun Zhang, Tianhao Wang, Michael Backes, Mathias Humbert, and Yang Zhang. Graph unlearning. In *Proceedings of the 2022 ACM SIGSAC Conference on Computer and Communications Security*, pages 499–513, 2022.

[8] Zhao Chen, Vijay Badrinarayanan, Chen-Yu Lee, and Andrew Rabinovich. Gradnorm: Gradient normalization for adaptive loss balancing in deep multitask networks. In *International conference on machine learning*, pages 794–803. PMLR, 2018.

[9] Zhao Chen, Jiquan Ngiam, Yanping Huang, Thang Luong, Henrik Kretzschmar, Yuning Chai, and Dragomir Anguelov. Just pick a sign: Optimizing deep multitask models with gradient sign dropout. *Advances in Neural Information Processing Systems*, 33:2039–2050, 2020.

[10] Jiali Cheng, George Dasoulas, Huan He, Chirag Agarwal, and Marinka Zitnik. Gnndelete: A general strategy for unlearning in graph neural networks. *arXiv preprint arXiv:2302.13406*, 2023.

[11] Eli Chien, Chao Pan, and Olgica Milenkovic. Certified graph unlearning. *arXiv preprint arXiv:2206.09140*, 2022.

[12] Ana Luísa Custódio, JF Aguilar Madeira, A Ismael F Vaz, and Luís Nunes Vicente. Direct multisearch for multiobjective optimization. *SIAM Journal on Optimization*, 21(3):1109–1140, 2011.

[13] Ashok Cutkosky and Francesco Orabona. Momentum-based variance reduction in non-convex sgd. *Advances in Neural Information Processing Systems*, 32, 2019.

[14] Jean-Antoine Désidéri. Multiple-gradient descent algorithm (mgda) for multiobjective optimization. *Comptes Rendus Mathematique*, 350(5-6):313–318, 2012.

[15] Yoel Drori and Ohad Shamir. The complexity of finding stationary points with stochastic gradient descent. In *International Conference on Machine Learning*, pages 2658–2667, 2020.

[16] Cynthia Dwork, Krishnaram Kenthapadi, Frank McSherry, Ilya Mironov, and Moni Naor. Our data, ourselves: Privacy via distributed noise generation. In *Annual international conference on the theory and applications of cryptographic techniques*, pages 486–503. Springer, 2006.

[17] Ronen Eldan and Mark Russinovich. Who's harry potter? approximate unlearning in llms. *arXiv preprint arXiv:2310.02238*, 2023.

[18] Chongyu Fan, Jiancheng Liu, Yihua Zhang, Dennis Wei, Eric Wong, and Sijia Liu. Salun: Empowering machine unlearning via gradient-based weight saliency in both image classification and generation. *arXiv preprint arXiv:2310.12508*, 2023.

[19] Heshan Devaka Fernando, Han Shen, Miao Liu, Subhajit Chaudhury, Keerthiram Murugesan, and Tianyi Chen. Mitigating gradient bias in multi-objective learning: A provably convergent approach. In *The Eleventh International Conference on Learning Representations*, 2023.

[20] Jörg Fliege, A Ismael F Vaz, and Luís Nunes Vicente. Complexity of gradient descent for multiobjective optimization. *Optimization Methods and Software*, 34(5):949–959, 2019.

[21] Matt Fredrikson, Somesh Jha, and Thomas Ristenpart. Model inversion attacks that exploit confidence information and basic countermeasures. In *Proceedings of the 22nd ACM SIGSAC conference on computer and communications security*, pages 1322–1333, 2015.

[22] Rohit Gandikota, Joanna Materzyńska, Jaden Fiotto-Kaufman, and David Bau. Erasing concepts from diffusion models. In *Proceedings of the 2023 IEEE International Conference on Computer Vision*, 2023.

[23] Antonio Ginart, Melody Guan, Gregory Valiant, and James Y Zou. Making ai forget you: Data deletion in machine learning. *Advances in neural information processing systems*, 32, 2019.

[24] Aditya Golatkar, Alessandro Achille, and Stefano Soatto. Eternal sunshine of the spotless net: Selective forgetting in deep networks. In *Proceedings of the IEEE/CVF Conference on Computer Vision and Pattern Recognition*, pages 9304–9312, 2020.

[25] Laura Graves, Vineel Nagisetty, and Vijay Ganesh. Amnesiac machine learning. In *Proceedings of the AAAI Conference on Artificial Intelligence*, volume 35, pages 11516–11524, 2021.

[26] Chuan Guo, Tom Goldstein, Awni Hannun, and Laurens Van Der Maaten. Certified data removal from machine learning models. *arXiv preprint arXiv:1911.03030*, 2019.

[27] Michelle Guo, Albert Haque, De-An Huang, Serena Yeung, and Li Fei-Fei. Dynamic task prioritization for multitask learning. In *Proceedings of the European conference on computer vision (ECCV)*, pages 270–287, 2018.

[28] Yifei He, Shiji Zhou, Guojun Zhang, Hyokun Yun, Yi Xu, Belinda Zeng, Trishul Chilimbi, and Han Zhao. Robust multi-task learning with excess risks. In *International Conference on Machine Learning (ICML)*, 2024.

[29] Jack Hessel, Ari Holtzman, Maxwell Forbes, Ronan Le Bras, and Yejin Choi. Clipscore: A reference-free evaluation metric for image captioning. *arXiv preprint arXiv:2104.08718*, 2021.

[30] Martin Heusel, Hubert Ramsauer, Thomas Unterthiner, Bernhard Nessler, and Sepp Hochreiter. Gans trained by a two time-scale update rule converge to a local nash equilibrium. *Advances in neural information processing systems*, 30, 2017.

[31] Jonathan Ho and Tim Salimans. Classifier-free diffusion guidance. *arXiv preprint arXiv:2207.12598*, 2022.

[32] Tuan Hoang, Santu Rana, Sunil Gupta, and Svetha Venkatesh. Learn to unlearn for deep neural networks: Minimizing unlearning interference with gradient projection. In *Proceedings of the IEEE/CVF Winter Conference on Applications of Computer Vision*, pages 4819–4828, 2024.

[33] Jeremy Howard and Sylvain Gugger. Fastai: A layered api for deep learning. *Information*, 11(2):108, 2020.

[34] Yuzheng Hu, Ruicheng Xian, Qilong Wu, Qiuling Fan, Lang Yin, and Han Zhao. Revisiting scalarization in multi-task learning: A theoretical perspective. *Advances in Neural Information Processing Systems*, 36, 2024.

[35] Mark He Huang, Lin Geng Foo, and Jun Liu. Learning to unlearn for robust machine unlearning. *arXiv preprint arXiv:2407.10494*, 2024.

[36] Ali Jadbabaie, Alexander Rakhlin, Shahin Shahrampour, and Karthik Sridharan. Online optimization: Competing with dynamic comparators. In *Artificial Intelligence and Statistics*, pages 398–406. PMLR, 2015.

[37] Adrián Javaloy and Isabel Valera. Rotograd: Gradient homogenization in multitask learning. *arXiv preprint arXiv:2103.02631*, 2021.

[38] Jinghan Jia, Jiancheng Liu, Parikshit Ram, Yuguang Yao, Gaowen Liu, Yang Liu, Pranay Sharma, and Sijia Liu. Model sparsification can simplify machine unlearning. *arXiv preprint arXiv:2304.04934*, 2023.

[39] Enkelejda Kasneci, Kathrin Seßler, Stefan Küchemann, Maria Bannert, Daryna Dementieva, Frank Fischer, Urs Gasser, Georg Groh, Stephan Günnemann, Eyke Hüllermeier, et al. Chatgpt for good? on opportunities and challenges of large language models for education. *Learning and individual differences*, 103:102274, 2023.

[40] Alex Kendall, Yarin Gal, and Roberto Cipolla. Multi-task learning using uncertainty to weigh losses for scene geometry and semantics. In *Proceedings of the IEEE conference on computer vision and pattern recognition*, pages 7482–7491, 2018.

[41] Nupur Kumari, Bingliang Zhang, Sheng-Yu Wang, Eli Shechtman, Richard Zhang, and Jun-Yan Zhu. Ablating concepts in text-to-image diffusion models. In *Proceedings of the IEEE/CVF International Conference on Computer Vision*, pages 22691–22702, 2023.

[42] Yunwen Lei, Ting Hu, Guiying Li, and Ke Tang. Stochastic gradient descent for nonconvex learning without bounded gradient assumptions. *IEEE Transactions on Neural Networks and Learning Systems*, 2020.

[43] Shen Lin, Xiaoyu Zhang, Willy Susilo, Xiaofeng Chen, and Jun Liu. Gdr-gma: Machine unlearning via direction-rectified and magnitude-adjusted gradients. In *Proceedings of the 32nd ACM International Conference on Multimedia*, MM '24, page 9087–9095, New York, NY, USA, 2024. Association for Computing Machinery.

[44] Bo Liu, Yihao Feng, Peter Stone, and Qiang Liu. Famo: Fast adaptive multitask optimization, 2023.

[45] Bo Liu, Yihao Feng, Peter Stone, and Qiang Liu. Famo: Fast adaptive multitask optimization. *Advances in Neural Information Processing Systems*, 36, 2024.

[46] Bo Liu, Xingchao Liu, Xiaojie Jin, Peter Stone, and Qiang Liu. Conflict-averse gradient descent for multi-task learning. *Advances in Neural Information Processing Systems*, 34:18878–18890, 2021.

[47] Sijia Liu, Yuanshun Yao, Jinghan Jia, Stephen Casper, Nathalie Baracaldo, Peter Hase, Xiaojun Xu, Yuguang Yao, Hang Li, Kush R Varshney, et al. Rethinking machine unlearning for large language models. *arXiv preprint arXiv:2402.08787*, 2024.

[48] Yi Liu, Lei Xu, Xingliang Yuan, Cong Wang, and Bo Li. The right to be forgotten in federated learning: An efficient realization with rapid retraining. *arXiv preprint arXiv:2203.07320*, 2022.

[49] Mengyao Lyu, Yuhong Yang, Haiwen Hong, Hui Chen, Xuan Jin, Yuan He, Hui Xue, Jungong Han, and Guiguang Ding. One-dimensional adapter to rule them all: Concepts, diffusion models and erasing applications. *arXiv preprint arXiv:2312.16145*, 2023.

[50] Pamela Mishkin, Lama Ahmad, Miles Brundage, Gretchen Krueger, and Girish Sastry. Dall· e 2 preview-risks and limitations. *Noudettu*, 28:2022, 2022.

[51] Seth Neel, Aaron Roth, and Saeed Sharifi-Malvajerdi. Descent-to-delete: Gradient-based methods for machine unlearning. In *Algorithmic Learning Theory*, pages 931–962. PMLR, 2021.

[52] Thanh Tam Nguyen, Thanh Trung Huynh, Phi Le Nguyen, Alan Wee-Chung Liew, Hongzhi Yin, and Quoc Viet Hung Nguyen. A survey of machine unlearning. *arXiv preprint arXiv:2209.02299*, 2022.

[53] Youyang Qu, Xin Yuan, Ming Ding, Wei Ni, Thierry Rakotoarivelo, and David Smith. Learn to unlearn: A survey on machine unlearning, 2023.

[54] Alec Radford, Jong Wook Kim, Chris Hallacy, Aditya Ramesh, Gabriel Goh, Sandhini Agarwal, Girish Sastry, Amanda Askell, Pamela Mishkin, Jack Clark, et al. Learning transferable visual models from natural language supervision. In *International conference on machine learning*, pages 8748–8763. PMLR, 2021.

[55] Robin Rombach, Andreas Blattmann, Dominik Lorenz, Patrick Esser, and Björn Ommer. High-resolution image synthesis with latent diffusion models. In *Proceedings of the IEEE/CVF conference on computer vision and pattern recognition*, pages 10684–10695, 2022.

[56] Patrick Schramowski, Manuel Brack, Björn Deiseroth, and Kristian Kersting. Safe latent diffusion: Mitigating inappropriate degeneration in diffusion models. In *Proceedings of the IEEE/CVF Conference on Computer Vision and Pattern Recognition*, pages 22522–22531, 2023.

[57] Ayush Sekhari, Jayadev Acharya, Gautam Kamath, and Ananda Theertha Suresh. Remember what you want to forget: Algorithms for machine unlearning. *Advances in Neural Information Processing Systems*, 34:18075–18086, 2021.

[58] Ozan Sener and Vladlen Koltun. Multi-task learning as multi-objective optimization. *Advances in neural information processing systems*, 31, 2018.

[59] Masahiro Suzuki and Yutaka Matsuo. A survey of multimodal deep generative models. *Advanced Robotics*, 36(5-6):261–278, 2022.

[60] Ayush K Tarun, Vikram S Chundawat, Murari Mandal, and Mohan Kankanhalli. Fast yet effective machine unlearning. *IEEE Transactions on Neural Networks and Learning Systems*, 2023.

[61] Anvith Thudi, Gabriel Deza, Varun Chandrasekaran, and Nicolas Papernot. Unrolling sgd: Understanding factors influencing machine unlearning. In *2022 IEEE 7th European Symposium on Security and Privacy (EuroS&P)*, pages 303–319. IEEE, 2022.

[62] Enayat Ullah, Tung Mai, Anup Rao, Ryan A Rossi, and Raman Arora. Machine unlearning via algorithmic stability. In *Conference on Learning Theory*, pages 4126–4142. PMLR, 2021.

[63] Junxiao Wang, Song Guo, Xin Xie, and Heng Qi. Federated unlearning via class-discriminative pruning. In *Proceedings of the ACM Web Conference 2022*, pages 622–632, 2022.

[64] Alexander Warnecke, Lukas Pirch, Christian Wressnegger, and Konrad Rieck. Machine unlearning of features and labels. *arXiv preprint arXiv:2108.11577*, 2021.

[65] Leijie Wu, Song Guo, Junxiao Wang, Zicong Hong, Jie Zhang, and Yaohong Ding. Federated unlearning: Guarantee the right of clients to forget. *IEEE Network*, 36(5):129–135, 2022.

[66] Yongliang Wu, Shiji Zhou, Mingzhuo Yang, Lianzhe Wang, Wenbo Zhu, Heng Chang, Xiao Zhou, and Xu Yang. Unlearning concepts in diffusion model via concept domain correction and concept preserving gradient. *arXiv preprint arXiv:2405.15304*, 2024.

[67] Tianbao Yang, Lijun Zhang, Rong Jin, and Jinfeng Yi. Tracking slowly moving clairvoyant: Optimal dynamic regret of online learning with true and noisy gradient. In *International Conference on Machine Learning*, pages 449–457. PMLR, 2016.

[68] Yuanshun Yao, Xiaojun Xu, and Yang Liu. Large language model unlearning. *arXiv preprint arXiv:2310.10683*, 2023.

[69] Tianhe Yu, Saurabh Kumar, Abhishek Gupta, Sergey Levine, Karol Hausman, and Chelsea Finn. Gradient surgery for multi-task learning. *Advances in Neural Information Processing Systems*, 33:5824–5836, 2020.

[70] Eric Zhang, Kai Wang, Xingqian Xu, Zhangyang Wang, and Humphrey Shi. Forget-me-not: Learning to forget in text-to-image diffusion models. *arXiv preprint arXiv:2303.17591*, 2023.

[71] Han Zhao, Jianfeng Chi, Yuan Tian, and Geoffrey J Gordon. Trade-offs and guarantees of adversarial representation learning for information obfuscation. *Advances in Neural Information Processing Systems*, 33:9485–9496, 2020.

[72] Han Zhao, Chen Dan, Bryon Aragam, Tommi S Jaakkola, Geoffrey J Gordon, and Pradeep Ravikumar. Fundamental limits and tradeoffs in invariant representation learning. *Journal of machine learning research*, 23(340):1–49, 2022.

[73] Peng Zhao, Guanghui Wang, Lijun Zhang, and Zhi-Hua Zhou. Bandit convex optimization in non-stationary environments. *Journal of Machine Learning Research*, 22(125):1–45, 2021.

[74] Wayne Xin Zhao, Kun Zhou, Junyi Li, Tianyi Tang, Xiaolei Wang, Yupeng Hou, Yingqian Min, Beichen Zhang, Junjie Zhang, Zican Dong, et al. A survey of large language models. *arXiv preprint arXiv:2303.18223*, 2023.

[75] Shiji Zhou, Lianzhe Wang, Jiangnan Ye, Yongliang Wu, and Heng Chang. On the limitations and prospects of machine unlearning for generative ai. *arXiv preprint arXiv:2408.00376*, 2024.

[76] Shiji Zhou, Wenpeng Zhang, Jiyan Jiang, Wenliang Zhong, Jinjie Gu, and Wenwu Zhu. On the convergence of stochastic multi-objective gradient manipulation and beyond. *Advances in Neural Information Processing Systems*, 35:38103–38115, 2022.

[77] Eckart Zitzler and Lothar Thiele. Multiobjective evolutionary algorithms: a comparative case study and the strength pareto approach. *IEEE Transactions on Evolutionary Computation*, 3(4):257–271, 1999.

A Related Work

Our primary focus is on addressing pivotal issue within MU - unlearning-retaining tradeoff. We will first compare our approach with existing MU methods, elucidating why current techniques fall short in resolving the targeted issues. Subsequently, we introduce the multi-objective optimization approach, which may offer solutions to the tradeoff problem. We will discuss the reasons why these methods cannot be directly applied to MU and propose our novel strategies to effectively tackle these complex problems.

Machine Unlearning (MU) aims to refine machine learning models by eradicating the impact of certain data points or classes, primarily to avert potential privacy violations post-training [23, 51, 62, 57]. The ideal of complete unlearning, akin to retraining from scratch, is computationally prohibitive despite its theoretical merits. To mitigate this, research has ventured into probabilistic techniques such as Differential Privacy (DP) [23, 26, 51, 62, 57]. Yet, these techniques encounter limitations that impede their efficacy, notably in thwarting membership inference attacks [16, 25]. Consequently, there is a pivot towards crafting more potent and economical MU strategies [24, 3, 61, 38, 6, 64]. The reach of MU has extended into federated learning [63, 48, 65] and graph neural networks [7, 11, 10], amplifying its utility in diverse data ecosystems. Nonetheless, current methodologies grapple with balancing unlearning effectiveness and model utility, alongside the adaptability of MU methods across varied scenarios. A pertinent work, SalUn [18], harnesses gradient information for parameter selection. However, most of current methods neglect the critical role of dispersing selected parameters across the network for thorough unlearning and fails to tackle the gradient conflict issue, a pivotal aspect of optimizing unlearning processes. It is noteworthy that some works [32, 35, 66] also adopt the technique of explicit unilateral gradient surgery. However, they are based on heuristic methods, while our paper provides the original optimization framework and theoretical support, which is quite different in terms of the principle origin. Also, the computational cost of explicit unilateral gradient surgery is almost double than EUPMU.

Concept erasure in diffusion models. Beyond discriminative MU, text-to-image diffusion erasure has emerged as a parallel line tackling the removal of artists/styles/instances. SPM introduces a one-dimensional, plug-and-play adapter with latent anchoring and input-dependent permeability for non-invasive multi-concept erasure [49]. ConAbl (Concept Ablation) matches the target distribution to an anchor concept to prevent generation of a specific style/instance while preserving related concepts [41]. ESD (Erasing Concepts from Diffusion Models) fine-tunes diffusion weights with negative guidance as teacher to permanently remove a concept [22]. Notably, SPM and ConAbl both optimize a *forget loss* and an optional *retain loss* via *linear* weighting. Our EUPMU view suggests recasting such objectives under an *explicit utility-loss constraint* (retain budget) while optimizing the unlearning objective—i.e., a constrained alternative to linear scalarization—which can be implemented by our implicit unilateral surgery in a single backprop and could directly boost this family of methods.

Other gradient-operation MU. Methods like GDR–GMA (using direction-rectified, magnitude-adjusted gradients) [43] and Learn to Unlearn [53] (manipulate gradients through projecting gradients away from a pre-computed Core Gradient Space (CGS) to mitigate conflicts) both use gradient related operations in MU. These are largely heuristic gradient corrections or projections, whereas our approach derives the *exact* surgery from an optimization principle (the Utility-Preserving Unlearning Problem) and exposes a user-specified utility budget for proactive, interpretable control. Our methods also could avoid extra calculation coming from gradient operation through efficient implicit gradient operation.

Multi-Objective Optimization (MOO) have been developed to address the concurrent learning of multiple tasks through gradient modulation. A common approach in these methods involves dynamically re-weighting objectives based on uncertainty metrics [40], gradient magnitudes [8], and the complexity of training tasks [27]. The structured design and stable training of Multi-Objective Optimization (MOO) strategies have attracted significant interest. For example, [58] framed Multi-Task Learning (MTL) within an MOO context, proposing an adaptation of the Multiple Gradient Descent Algorithm (MGDA) for the task. Several techniques have been introduced to resolve gradient conflicts. Notably, [69] developed PCGrad, which aligns each task's gradient within the norm plane of the others. GradDrop reduces conflict by stochastically dropping conflicting gradients [9], RotoGrad resolves conflicts through gradient rotation [37], and [46] introduced CAGrad, which

Algorithm 1 Efficient Utility-Preserving Machine Unlearning (EUPMU)

```
Input: Initial model parameter $\boldsymbol{\theta}_0 = \boldsymbol{\theta}_1$ to be a pre-trained model, initial retaining parameter $\lambda_0 = 0$, learning rate $\{\alpha_t, \beta_t\}_{t=1}^{T}$, error tolerance $\{\varepsilon_t\}_{t=1}^{T}$, unlearning loss $\ell_u(\cdot)$, maximum value $D$ for $\lambda_t$ and retaining loss $\ell_r(\cdot)$
1: for $t = 1, \ldots, T$ do
2:     Update retaining parameter $\lambda_t$ by Eq. 8 as
       $\tilde{\delta}_{t-1} = \frac{1}{\alpha_t}(\ell_r(\boldsymbol{\theta}_{t-1}) - \ell_r(\boldsymbol{\theta}_t)) + \varepsilon_{t-1}$
       $\lambda_t = \min\left\{D, \max\left\{0, \lambda_{t-1} - \beta_{t-1}\tilde{\delta}_{t-1}\right\}\right\}$
3:     Update direction $\boldsymbol{d}_t = \nabla_{\boldsymbol{\theta}_t}\left(\ell_u(\boldsymbol{\theta}_t) + \lambda_t \ell_r(\boldsymbol{\theta}_t)\right)$
4:     Perform gradient step $\boldsymbol{\theta}_{t+1} = \boldsymbol{\theta}_t - \alpha_t \boldsymbol{d}_t$
5: end for
```

constrains gradients within a localized region around the average gradient direction. These strategies primarily target deterministic scenarios. [19] advanced MoCo as a probabilistic counterpart to MGDA, providing a comprehensive convergence and complexity analysis. [44] is the efficient method for MGDA, which address the additional computation cost brought by MOO. However, as discussed in the main text, all the MOO methods fail to be directly applied to MU.

B Algorithmic Details

Note that the clipping operator of step 2 in Algorithm 1 is due to the fact that $\lambda_t \geq 0$ and the practical need for fear of parameter explosion.

C Missing Proofs

In this section, we present the proof details.

C.1 Description for Assumption

In this paper, we have the following assumptions.

Assumption C.1 (L-Lipschitz)**.** For the objective function f, there exists a constant $L > 0$ such that for all $\boldsymbol{x}, \boldsymbol{y} \in \mathbb{R}^d$,

$$\|f(\boldsymbol{x}) - f(y)\| \leq L\|\boldsymbol{x} - \boldsymbol{y}\|.$$

Assumption C.2 (G-smoothness)**.** The objective function f is differentiable and its gradient ∇f is G-Lipschitz continuous, i.e., there exists a constant $G > 0$ such that for all $\boldsymbol{x}, \boldsymbol{y} \in \mathbb{R}^d$,

$$\|\nabla f(\boldsymbol{x}) - \nabla f(\boldsymbol{y})\| \leq G\|\boldsymbol{x} - \boldsymbol{y}\|.$$

Assumption C.3 (Function is bounded by B)**.** The objective function f is bounded by B, i.e., there exists a constant $B > 0$ such that for all $\boldsymbol{x} \in \mathbb{R}^d$,

$$|f(\boldsymbol{x})| \leq B.$$

C.2 Proof of Proposition 3.1

Proof. To derive the dual objective of Problem 3, we start by constructing the Lagrangian function associated with the primal problem. The Lagrangian can be written as:

$$\mathcal{L}(\boldsymbol{d}_t, \lambda_t) = \nabla \ell_u(\boldsymbol{\theta}_t) \cdot \boldsymbol{d}_t - \frac{1}{2}\|\boldsymbol{d}_t\|^2 + \lambda_t\left(\varepsilon_t + \nabla \ell_r(\boldsymbol{\theta}_t) \cdot \boldsymbol{d}_t\right),$$

where $\lambda_t \geq 0$ is the Lagrange multiplier corresponding to the constraint in the primal problem.

To find the dual objective, we first need to minimize the Lagrangian with respect to $\boldsymbol{d}_t$. Taking the gradient of $\mathcal{L}$ with respect to $\boldsymbol{d}_t$ and setting it to zero, we have:

$$\nabla_{\boldsymbol{d}_t}\mathcal{L}(\boldsymbol{d}_t, \lambda_t) = \nabla \ell_u(\boldsymbol{\theta}_t) + \lambda_t \nabla \ell_r(\boldsymbol{\theta}_t) - \boldsymbol{d}_t = 0.$$

Solving for $\boldsymbol{d}_t$, we obtain:

$$\boldsymbol{d}_t = \nabla \ell_u(\boldsymbol{\theta}_t) + \lambda_t \nabla \ell_r(\boldsymbol{\theta}_t).$$

Substituting this back into the Lagrangian, we get the dual function:

$$\begin{aligned} L_t(\lambda_t) &= \mathcal{L}(\boldsymbol{d}_t, \lambda_t) \\ &= \nabla \ell_u(\boldsymbol{\theta}_t) \cdot (\nabla \ell_u(\boldsymbol{\theta}_t) + \lambda_t \nabla \ell_r(\boldsymbol{\theta}_t)) \\ &\quad - \frac{1}{2} \left\| \nabla \ell_u(\boldsymbol{\theta}_t) + \lambda_t \nabla \ell_r(\boldsymbol{\theta}_t) \right\|^2 + \lambda_t \varepsilon_t. \end{aligned}$$

Expanding and simplifying, the dual objective becomes:

$$L_t(\lambda_t) = \frac{1}{2} \left\| \nabla \ell_u(\boldsymbol{\theta}_t) + \lambda_t \nabla \ell_r(\boldsymbol{\theta}_t) \right\|^2 + \lambda_t \varepsilon_t,$$

which is the dual objective stated in Proposition 3.1. □

C.3 Proof of Proposition 3.2

Proof. To find the closed-form solution for the optimal direction $\boldsymbol{d}_t^*$, we first minimize the dual objective $L_t(\lambda_t)$ with respect to λ_t. Taking the derivative of $L_t(\lambda_t)$ with respect to λ_t and setting it to zero, we get:

$$\frac{\partial L_t(\lambda_t)}{\partial \lambda_t} = \nabla \ell_r(\boldsymbol{\theta}_t) \cdot (\nabla \ell_u(\boldsymbol{\theta}_t) + \lambda_t \nabla \ell_r(\boldsymbol{\theta}_t)) + \varepsilon_t = 0.$$

Solving for λ_t, we obtain:

$$\lambda_t^* = \frac{-\nabla \ell_r(\boldsymbol{\theta}_t) \cdot \nabla \ell_u(\boldsymbol{\theta}_t) - \varepsilon_t}{\left\| \nabla \ell_r(\boldsymbol{\theta}_t) \right\|^2}.$$

Substituting λ_t^* back into the expression for $\boldsymbol{d}_t$, we find the optimal update direction $\boldsymbol{d}_t^*$ as:

$$\boldsymbol{d}_t^* = \begin{cases} \nabla \ell_u(\boldsymbol{\theta}_t) + \lambda_t^* \nabla \ell_r(\boldsymbol{\theta}_t), & \text{if } \lambda_t^* > 0, \\ \nabla \ell_u(\boldsymbol{\theta}_t), & \text{if } \lambda_t^* \leq 0. \end{cases}$$

□

C.4 Demonstration of Remark 3.3

Proof. By the G-smoothness, we have

$$\begin{aligned} \ell_r(\boldsymbol{\theta}_{i+1}) - \ell_r(\boldsymbol{\theta}_i) &\leq -\alpha_i \boldsymbol{d}_i \nabla l_r(\boldsymbol{\theta}_i) + \frac{\alpha_i^2 G}{2} \|\boldsymbol{d}_i\|^2 \\ &\leq \alpha_i \varepsilon_i + \frac{\alpha_i^2 G}{2} \|\boldsymbol{d}_i\|^2 \\ &\lesssim \alpha_i \varepsilon_i \text{ (if } \alpha_i \text{ is sufficient small).} \end{aligned}$$

The last inequality is because if α_i is sufficient small, the the second term is much smaller than the first term, and hence can be ignored in the approximation. By summing up the above from 0 to $t-1$, we can get

$$\ell_r(\boldsymbol{\theta}_t) - \ell_r(\boldsymbol{\theta}_0) \lesssim \mathcal{O}\left(\sum_{i=1}^{t} \varepsilon_t \alpha_t \right).$$

We hence proof the Theorem. □

Remark. If we set $\sum_{i=1}^{t} \varepsilon_t \alpha_t \leq \varepsilon$, then the total loss ascent is bounded by ε, and hence the performance drop can be controlled.

C.5 Proof of Theorem 3.4

Our proof adopts the following approach. The process of solving for λ is equivalent to a gradient update with a dynamic function, and the essence of the theorem is to bound the dynamic regret. Therefore, we intend to draw on results from online gradient descent (OGD) for dynamic regret to prove the theorem, where the crucial requirement of using OGD property is whether the total functional variation is controllable. Hence, we initially present a lemma to demonstrate this.

Lemma C.4. *Under the same assumption as Theorem 3.4, we have the bound for the total functional variation for dual function*

$$\begin{aligned}&\sum_{i=0}^{t} \sup_{\lambda} |L_{i+1}(\lambda) - L_i(\lambda)| \\ \leq{}& (D+1)^3 G L^2 \sum_{i=0}^{t} \alpha_i + D \sum_{i=0}^{t} |\varepsilon_{i+1} - \varepsilon_i|\end{aligned}$$

Proof. By the definition of $L_i(\lambda)$, we have

$$\begin{aligned}&|L_{i+1}(\lambda) - L_i(\lambda)| \\ &= |\frac{1}{2} \|\nabla \ell_u(\boldsymbol{\theta}_{i+1}) + \lambda \nabla \ell_r(\boldsymbol{\theta}_{i+1})\|^2 + \lambda \varepsilon_{i+1} \\ &\quad - (\frac{1}{2} \|\nabla \ell_u(\boldsymbol{\theta}_i) + \lambda \nabla \ell_r(\boldsymbol{\theta}_i)\|^2 + \lambda \varepsilon_i)| \\ &= \frac{1}{2}(\nabla \ell_u(\boldsymbol{\theta}_{i+1}) + \nabla \ell_u(\boldsymbol{\theta}_i) + \lambda \nabla \ell_r(\boldsymbol{\theta}_{i+1}) + \lambda \nabla \ell_r(\boldsymbol{\theta}_i)) \cdot \\ &\quad (\nabla \ell_u(\boldsymbol{\theta}_{i+1}) - \nabla \ell_u(\boldsymbol{\theta}_i) + \lambda \nabla \ell_r(\boldsymbol{\theta}_{i+1}) - \lambda \nabla \ell_r(\boldsymbol{\theta}_i)) \\ &\quad + \lambda |\varepsilon_{i+1} - \varepsilon_i| \\ &\leq \alpha_i (\lambda+1)^3 G L^2 + \lambda |\varepsilon_{i+1} - \varepsilon_i|,\end{aligned}$$

where the last inequality is from the assumption of L-Lipschitz and G-smoothness, we know that $\|\nabla \ell_u(\boldsymbol{\theta}_{i+1}) + \nabla \ell_u(\boldsymbol{\theta}_i) + \lambda \nabla \ell_r(\boldsymbol{\theta}_{i+1}) + \lambda \nabla \ell_r(\boldsymbol{\theta}_i)\| \leq 2(L + \lambda L)$, and

$$\begin{aligned}&\|\nabla \ell_u(\boldsymbol{\theta}_{i+1}) - \nabla \ell_u(\boldsymbol{\theta}_i) + \lambda \nabla \ell_r(\boldsymbol{\theta}_{i+1}) - \lambda \nabla \ell_r(\boldsymbol{\theta}_i)\| \\ &\leq \|\nabla \ell_u(\boldsymbol{\theta}_{i+1}) - \nabla \ell_u(\boldsymbol{\theta}_i)\| + \|\lambda \nabla \ell_r(\boldsymbol{\theta}_{i+1}) - \lambda \nabla \ell_r(\boldsymbol{\theta}_i)\| \\ &\leq G \|\boldsymbol{\theta}_{i+1} - \boldsymbol{\theta}_i\| + \lambda G \|\boldsymbol{\theta}_{i+1} - \boldsymbol{\theta}_i\| \text{ (G-smooth)} \\ &= (\lambda+1) G \|\alpha_i \boldsymbol{d}_i\| \\ &= \alpha_i (\lambda+1) G \|\nabla \ell_u(\boldsymbol{\theta}_{i+1}) + \lambda \nabla \ell_r(\boldsymbol{\theta}_{i+1})\| \\ &\leq \alpha_i (\lambda+1) G (1+\lambda) L \quad \text{(L-Lipschitz)} \\ &= \alpha_i (\lambda+1)^2 G L.\end{aligned}$$

Hence, we can get

$$\begin{aligned}&\sum_{i=0}^{t} \sup_{\lambda} |L_{i+1}(\lambda) - L_i(\lambda)| \\ &\leq \sum_{i=0}^{t} \sup_{\lambda} (\alpha_i (\lambda+1)^3 G L^2 + \lambda |\varepsilon_{i+1} - \varepsilon_i|) \\ &\leq (D+1)^3 G L^2 + \sum_{i=0}^{t} D |\varepsilon_{i+1} - \varepsilon_i| \\ &= (D+1)^3 G L^2 \sum_{i=0}^{t} \alpha_i + D \sum_{i=0}^{t} |\varepsilon_{i+1} - \varepsilon_i|.\end{aligned}$$

We now finish the proof. □

We now present the previous results of OGD, which can be later used for the final proof.

Lemma C.5 (Theorem 3 [36])**.** *Denote the total funtional variation*

$$V_t^f = \sum_{i=1}^{t-1} \sup_x |f_{i+1}(x) - f_i(x)|.$$

Online Gradient Descent algorithms with stepsize $\alpha = \mathcal{O}({V_t^f}^{1/3} t^{-1/3})$ *running with* f *enjoy the following bound*

$$\sum_{i=1}^{t} (f_i(x_i) - f_i(x_i^*)) \leq \mathcal{O}({V_t^f}^{1/3} t^{2/3}).$$

With the above results, we now can proof the theorem

Proof. By setting $\sum_{i=0}^t \alpha_i \leq \mathcal{O}(1)$ and $\sum_{i=0}^t \varepsilon_i \leq \mathcal{O}(1)$, we know that

$$\sum_{i=0}^{t} \sup_\lambda |L_{i+1}(\lambda) - L_i(\lambda)| \leq \mathcal{O}(1).$$

From the algorithm 1, we know that the update of λ is the process of online gradient descent [67] with stepsize $\beta_i/\alpha_i = \mathcal{O}(1/t^{1/3})$. Using the result of Lemma C.5, we can get that

$$\begin{aligned}
&\sum_{i=1}^{t} (L_i(\lambda_i) - L_i(\lambda_i^*)) \\
&\leq \mathcal{O}((\sum_{i=0}^{t} \sup_\lambda |L_{i+1}(\lambda) - L_i(\lambda)|)^{1/3} t^{2/3}) \\
&\leq \mathcal{O}(t^{2/3})
\end{aligned}$$

Dividing both side by t, we finally have

$$\frac{1}{t} \sum_{i=1}^{t} (L_i(\lambda_i) - L_i(\lambda_i^*)) \leq \mathcal{O}(1/t^{1/3}).$$

We hence end the proof. □

Remark. It should be noted that the presented results pertain to the use of the true gradient of L_t, whereas an approximation of the true gradient is employed for the update of λ. However, this approximation is a two-point estimate of the true gradient, and prior research [73] has demonstrated that the dynamic regret associated with such an approximation is equivalent to that of OGD when using the true gradient. Therefore, for the sake of clarity and to avoid redundancy, we have omitted this detail in the presentation.

C.6 Proof of Theorem 3.5

This convergence proof parallels the approach to obtaining a dynamic regret bound. We adhere to the foundational concept from [76], initially establishing a bound for the static regret, followed by bounding the discrepancy between the static and dynamic regrets. The synthesis of these bounds culminates in the final theorem. Hence, we first present the following Lemma.

Lemma C.6. *Under the same assumption as Theorem 3.5, denote* $\mathcal{C}_{\lambda_i}(\boldsymbol{\theta}) = \ell_u(\boldsymbol{\theta}) + \lambda_i \ell_r(\boldsymbol{\theta})$*, algorithm 1 enjoys the following bound*

$$\begin{aligned}
&\sum_{i=1}^{t} \mathcal{C}_{\lambda_i}(\boldsymbol{\theta}_i) - \min_{\boldsymbol{\theta}} \sum_{i=1}^{t} \mathcal{C}_{\lambda_i}(\boldsymbol{\theta}^*) \\
&\leq B \sum_{i=0}^{t-1} \beta_i (\frac{2B}{\alpha} + \varepsilon_t) + \frac{1}{2\alpha} \|\boldsymbol{\theta}_0 - \boldsymbol{\theta}^*\|^2 + DB.
\end{aligned}$$

Proof. By the G-smoothness, we have

$$\begin{aligned}\mathcal{C}_{\lambda_t}(\boldsymbol{\theta}_{i+1}) &\le \mathcal{C}_{\lambda_i}(\boldsymbol{\theta}_i) - \alpha_i \boldsymbol{d}_i \cdot \nabla \mathcal{C}_{\lambda_i}(\boldsymbol{\theta}_i) + \frac{\alpha_i^2 G}{2}\|\boldsymbol{d}_i\|^2 \\ &= \mathcal{C}_{\lambda_i}(\boldsymbol{\theta}_i) - \alpha_i \|\boldsymbol{d}_i\|^2 + \frac{\alpha_i^2 G}{2}\|\boldsymbol{d}_i\|^2 \\ &\le \mathcal{C}_{\lambda_i}(\boldsymbol{\theta}_t) - \frac{\alpha_i}{2}\|\boldsymbol{d}_i\|^2.\end{aligned}$$

The last inequality is due to the fact that $\alpha_i G \le 1$. By the convexity of both function, we can know that

$$\mathcal{C}_{\lambda_i}(\boldsymbol{\theta}_t) \le \mathcal{C}_{\lambda_i}(\boldsymbol{\theta}^*) + \boldsymbol{d}_i \cdot (\boldsymbol{\theta}_i - \boldsymbol{\theta}^*).$$

Plug into the first inequality, we obtain

$$\begin{aligned}\mathcal{C}_{\lambda_i}(\boldsymbol{\theta}_{i+1}) &\le \mathcal{C}_{\lambda_i}(\boldsymbol{\theta}^*) + \boldsymbol{d}_i \cdot (\boldsymbol{\theta}_t - \boldsymbol{\theta}^*) - \frac{\alpha_i}{2}\|\boldsymbol{d}_i\|^2 \\ &= \mathcal{C}_{\lambda_i}(\boldsymbol{\theta}^*) + \frac{1}{2\alpha_i}(\|\boldsymbol{\theta}_i - \boldsymbol{\theta}^*\|^2 - \|\boldsymbol{\theta}_i - \boldsymbol{\theta}^* - \alpha_i \boldsymbol{d}_i\|^2) \\ &= \mathcal{C}_{\lambda_i}(\boldsymbol{\theta}^*) + \frac{1}{2\alpha_i}(\|\boldsymbol{\theta}_i - \boldsymbol{\theta}^*\|^2 - \|\boldsymbol{\theta}_{i+1} - \boldsymbol{\theta}^*\|^2).\end{aligned}$$

For any $\boldsymbol{\theta}$, we have

$$\begin{aligned}\mathcal{C}_{\lambda_{i+1}}(\boldsymbol{\theta}) - \mathcal{C}_{\lambda_i}(\boldsymbol{\theta}) &= (\lambda_{i+1} - \lambda_i)\ell_r(\boldsymbol{\theta}) \\ &\le \beta_i B |\tilde{\delta}_i|.\end{aligned}$$

We then can get

$$\begin{aligned}&\mathcal{C}_{\lambda_{i+1}}(\boldsymbol{\theta}_{i+1}) - \mathcal{C}_{\lambda_i}(\boldsymbol{\theta}^*) \\ &= \mathcal{C}_{\lambda_{i+1}}(\boldsymbol{\theta}_{i+1}) - \mathcal{C}_{\lambda_i}(\boldsymbol{\theta}_{i+1}) + \mathcal{C}_{\lambda_i}(\boldsymbol{\theta}_{i+1}) - \mathcal{C}_{\lambda_i}(\boldsymbol{\theta}^*) \\ &= \beta_i B |\tilde{\delta}_i| + \frac{1}{2\alpha_i}(\|\boldsymbol{\theta}_i - \boldsymbol{\theta}^*\|^2 - \|\boldsymbol{\theta}_{i+1} - \boldsymbol{\theta}^*\|^2).\end{aligned}$$

Let $\alpha_i = \alpha, i = 1, \dots, t$ to be constant, and we have

$$\begin{aligned}&\sum_{i=1}^{t} \mathcal{C}_{\lambda_i}(\boldsymbol{\theta}_i) - \sum_{i=1}^{t} \mathcal{C}_{\lambda_i}(\boldsymbol{\theta}^*) \\ &= \sum_{i=0}^{t-1} (\mathcal{C}_{\lambda_{i+1}}(\boldsymbol{\theta}_{i+1}) - \mathcal{C}_{\lambda_i}(\boldsymbol{\theta}^*)) + \mathcal{C}_{\lambda_0}(\boldsymbol{\theta}^*) - \mathcal{C}_{\lambda_t}(\boldsymbol{\theta}^*) \\ &\le \sum_{i=0}^{t-1} \beta_i B |\tilde{\delta}_i| + \frac{1}{2\alpha}(\|\boldsymbol{\theta}_0 - \boldsymbol{\theta}^*\|^2 - \|\boldsymbol{\theta}_t - \boldsymbol{\theta}^*\|^2) \\ &\quad + (\lambda_0 - \lambda_t)\ell_r(\boldsymbol{\theta}^*) \\ &\le \sum_{i=0}^{t-1} \beta_i B |\tilde{\delta}_i| + \frac{1}{2\alpha}(\|\boldsymbol{\theta}_0 - \boldsymbol{\theta}^*\|^2 - \|\boldsymbol{\theta}_t - \boldsymbol{\theta}^*\|^2) + DB \\ &\le B \sum_{i=0}^{t-1} \beta_i (GL + \varepsilon_i) + \frac{1}{2\alpha}\|\boldsymbol{\theta}_0 - \boldsymbol{\theta}^*\|^2 + DB.\end{aligned}$$

The second inequality is by the assumption that λ is bounded by D and functions are bounded by B, and the last inequality is by fact that

$$\begin{aligned}|\tilde{\delta}_i| &= |\frac{1}{\alpha}(\ell_r(\boldsymbol{\theta}_i) - \ell_r(\boldsymbol{\theta}_{i+1})) + \varepsilon_i| \\ &\le |\frac{1}{\alpha}(\ell_r(\boldsymbol{\theta}_i) - \ell_r(\boldsymbol{\theta}_{i+1}))| + \varepsilon_i \\ &\le \frac{1}{\alpha} G \|\boldsymbol{\theta}_i - \boldsymbol{\theta}_{i+1}\| + \varepsilon_i \\ &= \frac{1}{\alpha} G \alpha \|d_i\| + \varepsilon_i \\ &\le GL + \varepsilon_i.\end{aligned}$$

The second inequality is by the G-smoothness, and the last inequality is by L-Lipschitz assumption. We thus end the proof. □

With the bounded static regret, we also need to introduce the following lemma to bound the gap between static and dynamic regrets.

Lemma C.7. *Under the same assumption as Theorem 3.5, algorithm 1 enjoys the following bound*

$$\min_{\boldsymbol{\theta}^*}\sum_{i=1}^{t}\mathcal{C}_{\lambda_i}(\boldsymbol{\theta}^*)-\sum_{i=1}^{t}\min_{\boldsymbol{\theta}_t^*}\mathcal{C}_{\lambda_i}(\boldsymbol{\theta}_t^*)\le B\sum_{i=1}^{t}i\beta_i(\frac{2B}{\alpha}+\varepsilon_t)$$

Proof. Denote $\overline{\lambda}=\frac{1}{t}\sum_{i=1}^{t}\lambda_i$. By the optimality of $\boldsymbol{\theta}^*$, we can know that

$$\begin{aligned}
&\sum_{i=1}^{t}\mathcal{C}_{\lambda_i}(\boldsymbol{\theta}^*)-\sum_{i=1}^{t}\mathcal{C}_{\lambda_i}(\boldsymbol{\theta}_t^*)\\
&=t(\ell_u(\boldsymbol{\theta}^*)+\overline{\lambda}\ell_r(\boldsymbol{\theta}^*))-\sum_{i=1}^{t}\mathcal{C}_{\lambda_i}(\boldsymbol{\theta}_t^*)\\
&\le\sum_{i=1}^{t}\mathcal{C}_{\overline{\lambda}}(\boldsymbol{\theta}_t^*)-\sum_{i=1}^{t}\mathcal{C}_{\lambda_i}(\boldsymbol{\theta}_t^*)\\
&\le\sum_{i=1}^{t}(\overline{\lambda}-\lambda_i)l_r(\boldsymbol{\theta}_t^*)\\
&\le B\sum_{i=1}^{t}|\overline{\lambda}-\lambda_i|.
\end{aligned}$$

The first inequality is by the fact that $\ell_u(\boldsymbol{\theta}^*)+\overline{\lambda}\ell_r(\boldsymbol{\theta}^*)\le\mathcal{C}_{\overline{\lambda}}(\boldsymbol{\theta}_t^*)$ from the optimality of $\boldsymbol{\theta}^*$, and the last one is from the bounded function assumption. We next try to upper bound $\sum_{i=1}^{t}|\overline{\lambda}-\lambda_i|$, and have

$$\begin{aligned}
\sum_{i=1}^{t}|\overline{\lambda}-\lambda_i|&=\sum_{i=1}^{t}|\frac{1}{t}\sum_{j=1}^{t}(\lambda_j-\lambda_i)|\le\frac{1}{t}\sum_{i=1}^{t}\sum_{j=1}^{t}|\lambda_j-\lambda_i|\\
&=\frac{1}{t}\sum_{i=1}^{t}\sum_{j=1}^{i-1}|\lambda_j-\lambda_i|+\frac{1}{t}\sum_{i=1}^{t}\sum_{j=i}^{t}|\lambda_j-\lambda_i|\\
&\le\frac{2}{t}\sum_{i=1}^{t}\sum_{j=i}^{t}\sum_{l=i}^{j}|\lambda_l-\lambda_{l+1}|\\
&=\frac{2}{t}\sum_{i=1}^{t}\sum_{l=i}^{t}(t-l+1)|\lambda_l-\lambda_{l+1}|\le2\sum_{i=1}^{t}\sum_{l=i}^{t}|\lambda_l-\lambda_{l+1}|\\
&=2\sum_{l=1}^{t}l|\lambda_l-\lambda_{l+1}|\le2\sum_{l=1}^{t}l\beta_i|\tilde{\delta}_i|\le\sum_{i=1}^{t}i\beta_i(GL+\varepsilon_I).
\end{aligned}$$

We thus end the proof by

$$\sum_{i=1}^{t}\mathcal{C}_{\lambda_i}(\boldsymbol{\theta}^*)-\sum_{i=1}^{t}\mathcal{C}_{\lambda_i}(\boldsymbol{\theta}_t^*)\le B\sum_{i=1}^{t}i\beta_i(GL+\varepsilon_i).$$

□

We observe that the gap between static and dynamic regrets is controlled by the stability of λ, which is the advantage of the approximate algorithm compared with the explicit gradient surgery. We are now ready to present the final proof.

Proof. Combining the results from Lemma C.6 and Lemma C.7, we can obtain

$$\begin{aligned} &\sum_{i=1}^{t}\mathcal{C}_{\lambda_i}(\boldsymbol{\theta}_i) - \sum_{i=1}^{t}\mathcal{C}_{\lambda_i}(\boldsymbol{\theta}_t^*) \\ =& \sum_{i=1}^{t}\mathcal{C}_{\lambda_i}(\boldsymbol{\theta}_i) - \sum_{i=1}^{t}\mathcal{C}_{\lambda_i}(\boldsymbol{\theta}^*) + \sum_{i=1}^{t}\mathcal{C}_{\lambda_i}(\boldsymbol{\theta}^*) - \sum_{i=1}^{t}\mathcal{C}_{\lambda_i}(\boldsymbol{\theta}_t^*) \\ \leq& B\sum_{i=0}^{t}(i+1)\beta_i(GL+\varepsilon_i) + \frac{1}{2\alpha}\|\boldsymbol{\theta}_0 - \boldsymbol{\theta}^*\|^2 + DB. \end{aligned}$$

Setting $\alpha_i = \alpha \leq \mathcal{O}(1/G)$, $\sum_{i=0}^{t}(i+1)\beta_i \leq \mathcal{O}(1)$, and $\sum_{i=1}^{t}\varepsilon_i \leq \mathcal{O}(1)$, we get

$$\sum_{i=1}^{t}\mathcal{C}_{\lambda_i}(\boldsymbol{\theta}_i) - \sum_{i=1}^{t}\mathcal{C}_{\lambda_i}(\boldsymbol{\theta}_t^*) \leq \mathcal{O}(1).$$

Therefore, we finally have

$$\frac{1}{t}(\sum_{i=1}^{t}\mathcal{C}_{\lambda_i}(\boldsymbol{\theta}_i) - \sum_{i=1}^{t}\mathcal{C}_{\lambda_i}(\boldsymbol{\theta}_t^*)) \leq \mathcal{O}(1/t).$$

This averaging convergence scheme for can be transformed to the traditional one in Theorem 3.5 by output the average solution from $\boldsymbol{\theta}_i, i = 1, \ldots T$ [13, 42, 15]. This paper leaves out the transforming details. □

C.7 Demonstration of Remark 3.6

In the Theorem 3.5, we have demonstrated that EUPMU can converge to the Pareto optimal solution, that is,

$$\mathcal{C}(\boldsymbol{\theta}_t) - \min_{\boldsymbol{\theta}}\mathcal{C}(\boldsymbol{\theta}) \leq \mathcal{O}(1/t).$$

Then we can get

$$\mu_u l_u(\boldsymbol{\theta}_t) - \mu_u l_u(\boldsymbol{\theta}^*) + \mu_r l_r(\boldsymbol{\theta}_t) - \mu_r l_r(\boldsymbol{\theta}^*) \leq \mathcal{O}(1/t).$$

By the fact that $l_r(\boldsymbol{\theta}_t) \geq l_r(\boldsymbol{\theta}^*)$, we have

$$\mu_u l_u(\boldsymbol{\theta}_t) - \mu_u l_u(\boldsymbol{\theta}^*) \leq \mathcal{O}(1/t).$$

Combining with the results of the theorem in Remark 3.3, we can know that the converged solution satisfies the condition that the decrease of the retaining loss is controlled by

$$\ell_r(\boldsymbol{\theta}_t) - \ell_r(\boldsymbol{\theta}_0) \lesssim \mathcal{O}\left(\sum_{i=1}^{t}\varepsilon_t\alpha_t\right).$$

By the fact that $l_u(\boldsymbol{\theta}_t) \geq l_u\boldsymbol{\theta}^*)$, we finally get

$$\ell_r(\boldsymbol{\theta}^*) - \ell_r(\boldsymbol{\theta}_0) \lesssim \mathcal{O}\left(\sum_{i=1}^{t}\varepsilon_t\alpha_t\right).$$

C.8 Proof of Theorem 3.7

To prove the Theorem, we follow a similar procedure to that of multi-objective proofs [20], first establishing a local recursive inequality, and then bounding the sum of these inequalities.

Lemma C.8. *Assume that L_u is G-smooth. Let $\alpha_i \leq 1/G$. We have*

$$\|\boldsymbol{d}_i\|^2 \leq \frac{2}{\alpha_i}(\ell_u(\boldsymbol{\theta}_i) - \ell_u(\boldsymbol{\theta}_{i+1})) + 2\lambda_i\varepsilon_i.$$

Proof. By the G-smoothness, we have

$$\begin{aligned}\ell_u(\boldsymbol{\theta}_{i+1}) - \ell_u(\boldsymbol{\theta}_i) &\leq -\alpha_i \boldsymbol{d}_i \cdot \nabla \ell_u(\boldsymbol{\theta}_i) + \frac{\alpha_i^2 G}{2}\|\boldsymbol{d}_i\|^2 \\ &= -\alpha_i \|\boldsymbol{d}_i\|^2 + \frac{\alpha_i^2 G}{2}\|\boldsymbol{d}_i\|^2 - \alpha_i \lambda_i \nabla \ell_r(\boldsymbol{\theta}_i) \cdot \boldsymbol{d}_i \\ &\leq -\frac{\alpha_i}{2}\|\boldsymbol{d}_i\|^2 - \alpha_i \lambda_i \nabla \ell_r(\boldsymbol{\theta}_i) \cdot \boldsymbol{d}_i.\end{aligned}$$

The equation is by the fact that $\boldsymbol{d}_i = \nabla \ell_u(\boldsymbol{\theta}_i) + \lambda_i \nabla \ell_r(\boldsymbol{\theta}_i)$. The last inequality is by the parameter setting that $\alpha_i \leq 1/G$. Hence, dividing both side by $\alpha_i/2$, we have

$$\begin{aligned}\|\boldsymbol{d}_i\|^2 &\leq \frac{2}{\alpha_i}(\ell_u(\boldsymbol{\theta}_i) - \ell_u(\boldsymbol{\theta}_{i+1})) - 2\lambda_i \nabla \ell_r(\boldsymbol{\theta}_i) \cdot \boldsymbol{d}_i \\ &\leq \frac{2}{\alpha_i}(\ell_u(\boldsymbol{\theta}_i) - \ell_u(\boldsymbol{\theta}_{i+1})) + 2\lambda_i \varepsilon_i.\end{aligned}$$

The last inequality is from the closed from solution of λ_i, which lead to the fact that when $\lambda_i \neq 0$, then

$$\begin{aligned}& -\nabla \ell_r(\boldsymbol{\theta}_i) \cdot \boldsymbol{d}_i = -\nabla \ell_r(\boldsymbol{\theta}_i) \cdot (\nabla \ell_u(\boldsymbol{\theta}_i) + \lambda_i \nabla \ell_r(\boldsymbol{\theta}_i)) \\ &= -\nabla \ell_r(\boldsymbol{\theta}_i) \cdot (\nabla \ell_u(\boldsymbol{\theta}_i) - \frac{\nabla \ell_r(\boldsymbol{\theta}_t) \cdot \nabla \ell_u(\boldsymbol{\theta}_t) + \varepsilon_t}{\|\nabla \ell_r(\boldsymbol{\theta}_t)\|^2} \nabla \ell_r(\boldsymbol{\theta}_i)) \\ &= -\nabla \ell_r(\boldsymbol{\theta}_i) \cdot (\nabla \ell_u(\boldsymbol{\theta}_i) - \frac{\nabla \ell_r(\boldsymbol{\theta}_t) \cdot \nabla \ell_u(\boldsymbol{\theta}_t)}{\|\nabla \ell_r(\boldsymbol{\theta}_t)\|^2} \nabla \ell_r(\boldsymbol{\theta}_i)) + \varepsilon_t \\ &= \varepsilon_t,\end{aligned}$$

where last equation is because the dot product of $\nabla \ell_r(\boldsymbol{\theta}_i)$ and the projected gradient $\nabla \ell_u(\boldsymbol{\theta}_i) - \frac{\nabla \ell_r(\boldsymbol{\theta}_t) \cdot \nabla \ell_u(\boldsymbol{\theta}_t)}{\|\nabla \ell_r(\boldsymbol{\theta}_t)\|^2} \nabla \ell_r(\boldsymbol{\theta}_i)$ is zero. We hence prove the Lemma. □

Lemma C.9. *Denote that* $\boldsymbol{d}_i^n = \frac{1}{1+\lambda_i}\boldsymbol{d}_i$

$$\sum_{i=1}^{t} \|\boldsymbol{d}_i^n\|^2 \leq (\frac{2}{\alpha_1} + \frac{4}{\alpha_{t+1}})B + 2\sum_{i=1}^{t} \varepsilon_i$$

Proof. From Lemma C.8, we know that

$$\|\boldsymbol{d}_i\|^2 \leq \frac{2}{\alpha_i}(\ell_u(\boldsymbol{\theta}_i) - \ell_u(\boldsymbol{\theta}_{i+1})) + 2\lambda_i \varepsilon_i,$$

and hence

$$\|\boldsymbol{d}_i^n\|^2 \leq \frac{1}{(\lambda_i+1)^2}(\frac{2}{\alpha_i}(\ell_u(\boldsymbol{\theta}_i) - \ell_u(\boldsymbol{\theta}_{i+1})) + 2\lambda_i \varepsilon_i).$$

By the fact that $\lambda_i \geq 0$, we then get

$$\begin{aligned}\|\boldsymbol{d}_i^n\|^2 &\leq \frac{2}{\alpha_i}(\ell_u(\boldsymbol{\theta}_i) - \ell_u(\boldsymbol{\theta}_{i+1})) + 2\frac{1}{(\lambda_i+1)^2}\lambda_i \varepsilon_i \\ &\leq \frac{2}{\alpha_i}(\ell_u(\boldsymbol{\theta}_i) - \ell_u(\boldsymbol{\theta}_{i+1})) + 2\varepsilon_i.\end{aligned}$$

Rearranging the above inequality, we can further obtain

$$\begin{aligned}\|\boldsymbol{d}_i^n\|^2 &\leq \frac{2}{\alpha_i}\ell_u(\boldsymbol{\theta}_i) - \frac{2}{\alpha_{i+1}}\ell_u(\boldsymbol{\theta}_{i+1}) \\ &\quad + (\frac{2}{\alpha_{i+1}} - \frac{2}{\alpha_i})\ell_u(\boldsymbol{\theta}_{i+1}) + 2\varepsilon_i \\ &\leq \frac{2}{\alpha_i}\ell_u(\boldsymbol{\theta}_i) - \frac{2}{\alpha_{i+1}}\ell_u(\boldsymbol{\theta}_{i+1}) \\ &\quad + (\frac{2}{\alpha_{i+1}} - \frac{2}{\alpha_i})B + 2\varepsilon_i.\end{aligned}$$

By summing up the above, we have

$$\begin{aligned}\sum_{i=1}^{t}\|\boldsymbol{d}_i^n\|^2 &\leq \sum_{i=1}^{t}(\frac{2}{\alpha_i}\ell_u(\boldsymbol{\theta}_i)-\frac{2}{\alpha_{i+1}}\ell_u(\boldsymbol{\theta}_{i+1}))\\ &\quad + B\sum_{i=1}^{t}(\frac{2}{\alpha_{i+1}}-\frac{2}{\alpha_i})+2\sum_{i=1}^{t}\varepsilon_i\\ &= \frac{2}{\alpha_1}\ell_u(\boldsymbol{\theta}_1)-\frac{2}{\alpha_{t+1}}\ell_u(\boldsymbol{\theta}_{t+1})\\ &\quad + B(\frac{2}{\alpha_{t+1}}-\frac{2}{\alpha_1})+2\sum_{i=1}^{t}\varepsilon_i\\ &\leq (\frac{2}{\alpha_1}+\frac{4}{\alpha_{t+1}})B+2\sum_{i=1}^{t}\varepsilon_i.\end{aligned}$$

We thus end the proof. □

Proof. By setting $\alpha_i, i=1,\ldots,T$ to be constant such that $\alpha_i \leq 1/G$, and $\sum_{i=1}^{t}\varepsilon_i \leq \mathcal{O}(1)$, we can get from Lemma C.9 that

$$\sum_{i=1}^{t}\|\boldsymbol{d}_i^n\|^2 \leq \mathcal{O}(1).$$

Dividing both side by t, we obtain

$$\frac{1}{t}\sum_{i=1}^{t}\|\boldsymbol{d}_i^n\|^2 \leq \mathcal{O}(1/t).$$

Finally, we end the proof by

$$\begin{aligned}&\min_{i=1,\ldots,t}\min_{(\mu_u,\mu_r)\in\Delta_2}\|\mu_u\nabla\ell_u(\boldsymbol{\theta}_i)+\mu_r\nabla\ell_r(\boldsymbol{\theta}_i)\|\\ \leq &\sqrt{\min_{i=1,\ldots,t}\|\boldsymbol{d}_i^n\|^2} \leq \sqrt{\frac{1}{t}\sum_{i=1}^{t}\|\boldsymbol{d}_i^n\|^2} \leq \mathcal{O}(1/t^{1/2}).\end{aligned}$$

□

D Additional Experimental Details and Results

We provide the experimental details and additional results in this section.

Average Gap (Avg.gap). Unless otherwise stated, all classification tables report the gap to retrain in the parentheses after each metric and **Avg.gap** in the last column defined as

$$\text{Avg.gap} = \frac{1}{4}\Big(|\text{UA}-\text{UA}_{\text{retrain}}|+|\text{RA}-\text{RA}_{\text{retrain}}|+|\text{TA}-\text{TA}_{\text{retrain}}|+|\text{MIA}-\text{MIA}_{\text{retrain}}|\Big),$$

computed on the same test split as the retrained reference. Lower is better.

Common protocols and configs. To avoid redundancy across 20+ runs, we follow the default hyperparameter templates from prior work and release the configuration files/command in our code repository. For classification, the MIA setup, train/val/test splits, and metric computation follow SalUn. For concept selection in style/instance experiments, the anchor concept protocol matches SPM. We include the search ranges in Appx. D.1 for reproducibility.

D.1 Additional training and unlearning settings

MU for image classification For image classification, we use *Unlearning Accuracy (UA)* and *Membership Inference Attack (MIA)* for unlearning efficacy, *Remaining Accuracy (RA)* and *Testing Accuracy (TA)* for classifier fidelity, and *Runtime Efficiency (RTE)* for computational efficiency in MU. The RTE is measured by relative overall runtime through the whole unlearning. To report overall performance succinctly, we use the **average gap (Avg.gap)**, defined as the mean absolute difference from a fully retrained model across {UA, RA, TA, MIA}, so lower is better. Our experiments encompass unlearning baselines, including FT [64], RL [24], GA [24], IU [61], ℓ_1-sparse [38], boundary unlearning BS/BE [6], SalUn [18], and gradient-operation unlearning GDR-GMA [43]. GDR-GMA uses direction-rectified and magnitude-adjusted gradients to update the retain and unlearning loss.

Training for both FT and RL methods occurs over 10 epochs to search for optimal learning rate within [1e-4, 1e-2]. Both GA and GDR-GMA use a 5-epoch learning rate search within [1e-6, 1e-3]. For IU, the parameter α related to the woodfisher Hessian Inverse approximation is explored between [1, 20]. ℓ_1-sparse involves a learning rate search for γ within [1e-6, 1e-4], while keeping a constant rate of 0.1. In the BS method, the FGSM step size is set to 0.1. Both BS and BE methods include a 10-epoch learning rate search within [1e-6, 1e-4]. SalUn and SalUn-soft are trained for 10 epochs with a fixed saliency map ratio of 0.5 and searched for the optimal learning rate with in [0.1, 1e-4]. Both EUPMU and EUPMU-fast using both unlearning and retain tasks for the optimization target, β within [0.01, 1] and then searched for ε within [1e-3, 5e-1].

For the ablation experiment, RL and EUPMU remain the same settings. FAMO is searched with weight learning rate from 1e-4 to 3e-2. PCGrad is searched learning rate within [1e-4, 1e-2]. Unilateral Gradient Surgery, also using log loss as the optimization target for both unlearning and retain tasks, under fixed learning rate 6e-5, is searched for ε within [1e-3, 5e-1]. Here the RTE is measured by one single epoch runtime under different MOO methods.

MU for image generation For DDPM, the forgetting settings are as follows: The batch size is set to 128. For EUPMU, it is trained for 1,000 iterations with a learning rate of 1e-4, an α value of 1e-3, and a batch size of 128. The sampling settings include 1,000 timesteps and a conditional scaling of 2.0. β is searched within [1e-4, 1e-2] and ε is searched within [1e+1, 5e+3]

For SD, the forgetting settings are as follows: For EUPMU, it is trained with the Adam optimizer for 5 epochs at a learning rate of 1e-5. The α value is set to 0.01, and the batch size is 8. The β is set to 1e-4 and ε is set to 1e+3 The sampling settings use DDIM with 100 timesteps and a conditional scaling of 7.5.

MU for Instance removing We employ ChatGPT to create 200 prompts $\{c\}$ containing the anchor concept, such as *"Dog"*. Following a similar process to the style pipeline, we generate 1000 images using the pre-trained diffusion model and obtain the target text prompts $\{c^*\}$ by substituting the word *"Dog"* with *"Snoopy"*.

MU for Style removing To remove style concept, we employ generic painting styles as an anchor concept in the process of style removal. Firstly, clip-retrieval [2] is used to obtain a set of text prompts $\{c\}$ that are close to the term *"painting"* in the CLIP latent space. Then, 1000 images are generated from the original model with 200 prompts. The target prompts $\{c^*\}$ are derived by appending the suffix *"in the style of {target style}"* to $\{c\}$.

MU for NSFW removing To remove NSFW content, we started by generating 800 images as $\boldsymbol{d}_f$ using SD V1.4 with the prompt "a photo of a nude person," and another 800 images as $\boldsymbol{d}_r$ with the prompt "a photo of a person wearing clothes." In the forgetting process, we treated "a photo of a nude person" as the concept to be forgotten and "a photo of a person wearing clothes" as the corrective remain concept. The settings for EUPMU remains identical to SD

D.2 More Details of Metrics

To assess the model's ability to unlearn the target concept and retain the generation capability, we utilize three key metrics: CLIP Score (CS), CLIP Accuracy (CA) [29] and Fréchet inception

Table 6: Results of class-wise forgetting for various methods of unlearning Resnet 18 for Cifar 10 classification. The result in the table is the mean value over 10 independent trials. The best unlearning performance for each forgetting class is highlighted in **bold**.

Methods	UA	RA	TA	MIA	Avg. Gap	Runtime
Retrain	100	100	94.68	100	0	-
FT	98.49 (1.51)	97.09 (2.91)	91.43 (3.25)	100.00 (0.00)	1.92	2.28
RL	98.44 (1.56)	96.88 (3.12)	90.97 (3.71)	100.00 (0.00)	2.10	2.45
GA	98.18 (1.82)	81.47 (18.53)	76.99 (17.69)	97.89 (2.11)	10.04	0.13
IU	98.33 (1.67)	95.00 (5.00)	89.19 (5.49)	99.42 (0.58)	3.19	3.25
BE	93.80 (6.20)	98.28 (1.72)	92.38 (2.30)	99.58 (0.42)	2.66	0.25
BS	92.24 (7.76)	96.75 (3.25)	91.03 (3.65)	98.82 (1.18)	3.96	0.41
ℓ_1-sparse	96.47 (3.53)	98.18 (1.82)	92.56 (2.12)	100.00 (0.00)	1.87	2.29
SalUn	98.00 (2.00)	99.91 (0.09)	**94.90 (0.22)**	100.00 (0.00)	0.58	2.46
SalUn-soft	98.96 (1.04)	99.75 (0.25)	94.41 (0.27)	100.00 (0.00)	0.39	2.50
GDRGMA	95.30 (4.70)	**100.00 (0.00)**	88.70 (5.98)	100.00 (0.00)	2.67	3.47
EUPMU	**99.64 (0.36)**	99.69 (0.31)	94.29 (0.39)	100.00 (0.00)	**0.27**	2.82
EUPMU-fast	98.18 (1.82)	99.83 (0.17)	94.36 (0.32)	100.00 (0.00)	0.58	2.52

Table 7: Results of Random Data Forgetting(10%) for various methods of unlearning Resnet 18 for Cifar 10 classification. The results are the mean value over 10 independent trials. The best performance is highlighted in **bold**.

Methods	UA	RA	TA	MIA	Avg. Gap
Retrain	5.24	100.00	94.26	12.88	0.00
FT	2.76 (2.48)	98.51 (1.49)	92.28 (1.98)	7.13 (5.75)	2.92
RL	3.27 (1.97)	**99.89 (0.11)**	**94.10 (0.16)**	23.73 (10.85)	3.27
GA	2.29 (2.95)	98.67 (1.33)	92.34 (1.92)	3.78 (9.10)	3.83
IU	0.56 (4.68)	99.51 (0.49)	94.58 (0.32)	1.02 (11.86)	4.34
BE	2.80 (2.44)	97.28 (2.72)	90.96 (3.30)	19.96 (7.08)	3.88
BS	0.71 (4.53)	99.24 (0.76)	93.64 (0.62)	13.64 (0.76)	1.67
ℓ_1-sparse	3.55 (1.69)	99.17 (0.83)	91.36 (2.90)	9.09 (3.79)	2.30
SalUn	5.02 (0.22)	99.83 (0.17)	93.58 (0.68)	27.38 (14.50)	3.89
SalUn-soft	**5.36 (0.12)**	99.71 (0.29)	93.29 (0.97)	24.53 (11.65)	3.26
GDRGMA	5.42 (0.18)	99.53 (0.47)	92.21 (2.05)	34.61 (21.73)	6.11
EUPMU	3.71 (1.53)	99.25 (0.75)	93.09 (1.17)	**12.89 (0.01)**	**0.86**
EUPMU-fast	3.64 (1.60)	99.54 (0.46)	93.17 (1.09)	13.29 (0.41)	0.89

distance (FID) [30]. After generating images with the big artists prompts from ESD [22] for art style unlearning and templates prompt proposed by CLIP [54], calculates the cosine similarity between the generated image and the target concept text embedding(e.g., "A quiet moment in Rembrandt's interior scene" or "Snoopy"). Likewise, CLIP Accuracy evaluates performance on a binary classification task distinguishing between the unlearning and retain concepts for each generated image, based on comparison of Clip Score. In both cases, lower metric values signify more effective concept ablation, while higher metrics indicate better retain of concept. Fréchet inception distance (FID) is a metric used to evaluate the quality and diversity of image generation. We use it to measure the similarity between the images by original Stable Diffusion model and our models' generated data distributions by comparing the mean and covariance of features extracted from a pretrained Inception-v3 model. A low FID indicates a similar distribution of two groups of image and better generation quality, while high FID refers to better unlearning result.

D.3 Additional Results and Demonstrations

Random Data Forgetting in Image Classification. Tables 7, 8, 9, 10, 11, 12, 13, 14, and 15 report random-data forgetting results. *Numbers in parentheses are the absolute gap to the retrain model for that metric.* Across CIFAR-10, CIFAR-100, and Tiny-ImageNet-200, the "Avg.gap" column quantifies the mean distance between each method and an ideal retrain; smaller is better. Our method yields consistently lower Avg.gap across forgetting ratios, indicating a favorable trade-off between forgetting efficacy and utility retention, in line with our algorithmic design and theory.

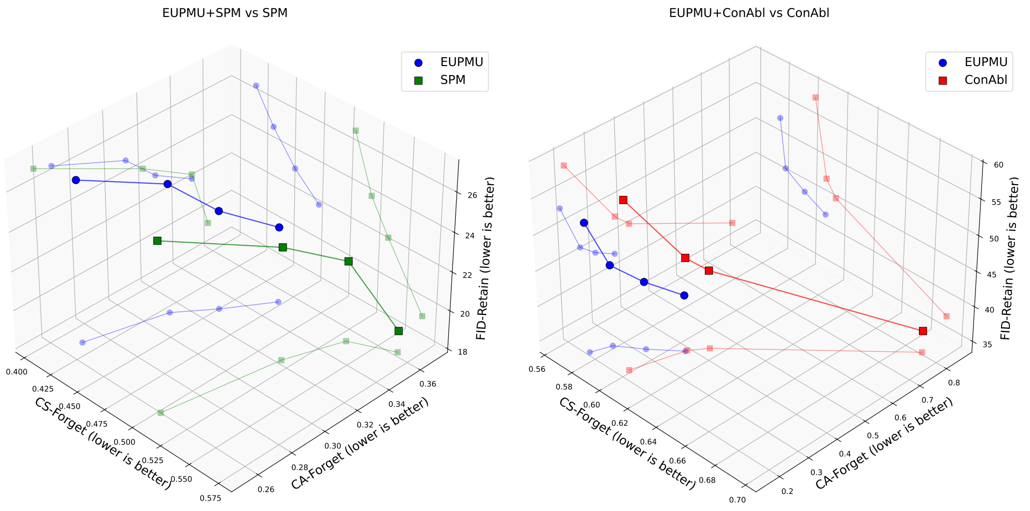

(a) SPM (b) ConAbl

Figure 6: Illustration of Pareto Front Analysis. We conducted comparative analyses by integrating EUPMU with SPM and ConAbl forgetting paradigms: (a) We compare EUPMU+SPM with pure SPM; (b) We compare EUPMU+ConAbl with pure ConAbl.

Table 8: Results of Random Data Forgetting(30%) for various methods of unlearning Resnet 18 for Cifar 10 classification. The results are the mean value over 10 independent trials. The best performance is highlighted in **bold**.

Methods	UA	RA	TA	MIA	Avg. Gap
Retrain	6.50	99.99	92.68	14.44	0.00
FT	4.93 (1.57)	96.89 (3.10)	90.75 (1.93)	11.10 (3.34)	2.48
RL	5.20 (1.30)	**99.68 (0.31)**	92.11 (0.57)	33.35 (18.91)	5.27
GA	0.50 (6.00)	99.48 (0.51)	94.64 (1.96)	1.07 (13.37)	5.46
IU	4.99 (1.51)	94.97 (5.02)	88.74 (3.94)	7.64 (6.80)	4.32
BE	0.59 (5.91)	98.82 (1.17)	93.89 (1.21)	8.19 (6.25)	3.63
BS	0.63 (5.87)	99.46 (0.53)	94.15 (1.47)	7.26 (7.18)	3.76
ℓ_1-sparse	4.76 (1.74)	97.30 (2.69)	91.26 (1.42)	10.36 (4.08)	2.48
SalUn	4.79 (1.71)	99.53 (0.46)	91.89 (0.79)	28.08 (13.64)	4.15
SalUn-soft	4.43 (2.07)	99.62 (0.37)	**92.42 (0.26)**	25.38 (10.94)	3.41
GDRGMA	**6.57 (0.07)**	99.53 (0.46)	91.79 (0.89)	38.41 (23.97)	6.35
EUPMU	3.53 (2.97)	98.34 (1.65)	91.80 (0.88)	16.50 (2.06)	1.89
EUPMU-fast	5.01 (1.49)	98.04 (1.95)	91.47 (1.21)	**16.19 (1.75)**	**1.60**

Class-wise Forgetting in Image Classification As shown in Table 6, cross all 10 categories' class-wise unlearning, our experiments consistently yielded results that align with the findings reported in the paper. Table 6 further details the performance for class-wise forgetting, where the metrics and the absolute gap are shown and the "Avg. Gap" column represents the average performance difference across unlearned (UA, RA, TA, MIA) and retrained models.

Visualization of Class-wise Forgetting in Image Classification Figure 7 demonstrates the Visualization of Class-wise Forgetting in Image Classification. Our analysis reveals that compared with baseline methods, EUPMU effectively enhances the erasure performance for target classes while preserving the capability to generate other classes. This observation is corroborated by the quantitative results presented in Table 5.

Table 9: Results of Random Data Forgetting(50%) for various methods of unlearning Resnet 18 for Cifar 10 classification. The results are the mean value over 10 independent trials. The best performance is highlighted in **bold**.

Methods	UA	RA	TA	MIA	Avg. Gap
Retrain	8.11	100.00	91.24	19.72	0.00
FT	2.84 (5.27)	98.75 (1.25)	91.87 (0.63)	7.35 (12.37)	4.88
RL	5.84 (2.27)	99.39 (0.61)	90.69 (0.55)	43.32 (23.60)	6.76
GA	0.62 (7.49)	99.40 (0.60)	94.49 (3.25)	1.23 (18.49)	7.46
IU	**7.57 (0.54)**	92.12 (7.88)	86.15 (5.09)	12.36 (7.36)	5.22
BE	10.69 (2.58)	89.72 (10.28)	82.88 (8.36)	22.72 (3.00)	6.05
BS	10.63 (2.52)	87.43 (12.57)	80.59 (10.65)	22.61 (2.89)	7.16
ℓ_1-sparse	1.27 (6.84)	93.39 (6.61)	98.69 (7.45)	9.49 (10.23)	7.78
SalUn	5.24 (2.87)	99.15 (0.85)	90.94 (0.30)	36.76 (17.04)	5.26
SalUn-soft	5.67 (2.44)	98.91 (1.09)	90.85 (0.39)	38.30 (18.58)	5.62
GDRGMA	4.46 (3.65)	**99.60 (0.40)**	91.68 (0.44)	36.51 (16.79)	5.32
EUPMU	4.71 (3.40)	96.96 (3.04)	90.35 (0.89)	19.55 (0.17)	1.88
EUPMU-fast	4.08 (4.03)	98.02 (1.98)	**91.11 (0.13)**	**19.84 (0.12)**	**1.56**

Table 10: Results of Random Data Forgetting(10%) for various methods of unlearning Resnet 18 for Cifar 100 classification. The results are the mean value over 10 independent trials. The best performance is highlighted in **bold**.

Methods	UA	RA	TA	MIA	Avg. Gap
Retrain	23.07	99.97	74.43	49.29	0.00
FT	6.07 (17.00)	98.45 (1.52)	71.44 (2.99)	17.56 (31.73)	13.31
RL	24.82 (1.75)	98.92 (1.05)	69.50 (4.93)	71.60 (22.31)	7.51
GA	4.16 (18.91)	96.90 (3.07)	**74.37 (0.06)**	8.62 (40.67)	15.68
IU	10.58 (12.49)	90.32 (9.65)	65.92 (8.51)	17.36 (31.93)	15.64
BE	3.40 (19.67)	96.72 (3.25)	71.58 (2.85)	13.58 (35.71)	15.37
BS	3.23 (19.84)	96.41 (3.56)	72.11 (2.32)	12.61 (36.68)	15.60
ℓ_1-sparse	2.40 (20.67)	98.14 (1.83)	75.85 (1.42)	7.31 (41.98)	16.48
SalUn	24.84 (1.77)	99.27 (0.70)	69.57 (4.86)	77.96 (28.67)	9.00
SalUn-soft	**24.73 (1.66)**	98.73 (1.24)	69.39 (5.04)	70.76 (21.47)	7.35
GDRGMA	56.67 (33.60)	**99.63 (0.34)**	68.74 (5.69)	93.71 (44.42)	21.01
EUPMU	9.67 (13.40)	99.60 (0.37)	72.03 (2.40)	**51.76 (2.47)**	**4.66**
EUPMU-fast	28.36 (5.29)	98.82 (1.15)	69.50 (4.93)	70.36 (21.07)	8.11

E Pareto Front Analysis

To quantitatively demonstrate EUPMU's enhanced trade-off balancing capability, we conducted comparative analyses by integrating EUPMU with SPM and ConAbl forgetting paradigms, followed by Pareto superiority evaluations against baseline methods. Specifically, following the experimental configuration for Style Unlearning as described in the main text, we performed style erasure on Van Gogh's artistic style while quantifying three performance metrics: (1 & 2) CS-forget and CA-Forget: CS and CA scores for Van Gogh style erasure efficacy, and (3) FID-Retain: FID score for Picasso style preservation. This tripartite evaluation framework provides analytical support for EUPMU's superior trade-off performance through comparative analysis of these interrelated metrics.

Figure 6 presents comprehensive experimental validation, demonstrating that integration with EUPMU enables SPM and ConAbl to achieve consistent improvements across all evaluated metrics, thereby yielding superior trade-off optimization outcomes. This empirical evidence indicates that EUPMU's optimization mechanism can effectively identify Pareto-optimal solutions through its enhanced search capabilities, aligning with the theoretical conclusions discussed in the main text.

Table 11: Results of Random Data Forgetting(30%) for various methods of unlearning Resnet 18 for Cifar 100 classification. The results are the mean value over 10 independent trials. The best performance is highlighted in **bold**.

Methods	UA	RA	TA	MIA	Avg. Gap
Retrain	29.00	99.97	71.47	52.22	0.00
FT	**30.27 (1.27)**	82.62 (17.35)	61.14 (10.33)	31.93 (20.29)	12.31
RL	26.14 (2.86)	98.12 (1.85)	63.46 (8.01)	66.68 (14.46)	6.79
GA	3.07 (25.93)	97.45 (2.52)	75.24 (3.77)	6.90 (45.32)	19.39
IU	10.82 (18.18)	90.43 (9.54)	65.30 (6.17)	17.50 (34.72)	17.15
BE	3.00 (26.00)	97.24 (2.73)	**73.68 (2.21)**	9.64 (42.58)	18.38
BS	2.95 (26.05)	97.32 (2.65)	73.81 (2.34)	8.84 (43.38)	18.61
ℓ_1-sparse	2.57 (26.43)	97.96 (2.01)	75.96 (4.49)	6.17 (46.05)	19.75
SalUn	24.08 (4.92)	98.19 (1.78)	61.74 (9.73)	65.16 (12.94)	7.34
SalUn-soft	25.39 (3.61)	97.59 (2.38)	62.12 (9.35)	62.49 (10.27)	6.40
GDRGMA	27.04 (1.96)	98.37 (1.60)	60.90 (10.57)	70.29 (18.07)	8.05
EUPMU	17.68 (11.32)	**98.96 (1.01)**	68.46 (3.01)	**50.93 (1.29)**	**4.16**
EUPMU-fast	19.64 (9.36)	97.81 (2.16)	62.53 (8.94)	56.06 (3.84)	6.08

Table 12: Results of Random Data Forgetting(50%) for various methods of unlearning Resnet 18 for Cifar 100 classification. The results are the mean value over 10 independent trials. The best performance is highlighted in **bold**.

Methods	UA	RA	TA	MIA	Avg. Gap
Retrain	33.28	99.98	67.75	61.21	0.00
FT	20.84 (12.44)	91.03 (8.95)	64.04 (3.71)	30.20 (31.01)	14.03
RL	22.48 (10.80)	95.51 (4.47)	54.52 (13.23)	53.41 (7.80)	9.07
GA	2.59 (30.69)	97.53 (2.45)	75.38 (7.63)	6.07 (55.14)	23.98
IU	6.76 (26.52)	93.58 (6.40)	**67.80 (0.05)**	13.06 (48.15)	20.28
BE	5.92 (27.36)	94.28 (5.70)	67.00 (0.75)	17.13 (44.08)	19.47
BS	6.22 (27.06)	94.54 (5.44)	66.62 (1.13)	16.57 (44.64)	19.57
ℓ_1-sparse	2.48 (30.80)	98.76 (1.22)	75.94 (8.19)	6.59 (54.62)	23.71
SalUn	**28.56 (4.72)**	96.31 (3.67)	52.88 (14.87)	**62.88 (1.67)**	6.23
SalUn-soft	24.84 (8.44)	95.44 (4.54)	54.32 (13.43)	55.50 (5.71)	8.03
GDRGMA	22.66 (10.62)	95.48 (4.50)	53.34 (14.41)	53.33 (7.88)	9.35
EUPMU	21.57 (11.71)	**98.97 (1.01)**	64.13 (3.62)	58.43 (2.78)	**4.78**
EUPMU-fast	18.68 (14.60)	94.20 (5.78)	54.29 (13.46)	40.91 (20.30)	13.54

F Limitations

While the proposed method demonstrates significant improvements over existing unlearning approaches, two inherent constraints persist: 1) Theoretically, we aim to achieve Pareto-optimal solutions that balance unlearning and utility objectives through error tolerance (ε_t) calibration. However, the absence of explicit patterns in these dual objectives prevents the formal derivation of their interrelationship within theoretical frameworks. Rigorous mathematical formulation would require introducing domain-specific assumptions about objective correlations, which inherently narrows the theoretical applicability. After careful consideration, we maintain the original formulation to preserve methodological generality; 2) Practically, the non-zero error tolerance $varepsilon_t \neq 0$ directly governs the trade-off between utility preservation and unlearning completeness. As shown in our ablation studies (Figure 6), this hyperparameter critically determines empirical performance. Nevertheless, lacking theoretical guidance for optimal ε_t, practical implementation relies on empirical tuning through grid search or Bayesian optimization. This dual constraint–theoretical indeterminacy and empirical dependency–defines the current practical boundary of our framework.

G Broader Impacts

This paper addresses the core unlearning-utility tradeoff in machine unlearning, aiming to enhance its practical deployability while effectively mitigating challenges posed by generative models producing

Table 13: Results of Random Data Forgetting(10%) for various methods of unlearning Resnet 18 for Tiny-Imagenet classification. The results are the mean value over 10 independent trials. The best performance is highlighted in **bold**.

Methods	UA	RA	TA	MIA	Avg. Gap
Retrain	36.54	99.98	63.71	64.57	0.00
FT	6.89 (29.65)	**98.80 (1.18)**	65.05 (1.34)	16.11 (48.46)	20.16
RL	28.40 (8.14)	98.35 (1.63)	61.17 (2.54)	**57.80 (6.77)**	4.77
GA	5.42 (31.12)	95.10 (4.88)	65.91 (2.20)	14.46 (50.11)	22.08
IU	11.79 (24.75)	89.83 (10.15)	61.37 (2.34)	14.98 (49.59)	21.71
BE	6.32 (30.22)	93.92 (6.06)	**63.99 (0.28)**	15.33 (49.24)	21.45
BS	6.28 (30.26)	93.96 (6.02)	64.15 (0.44)	15.50 (49.07)	21.45
ℓ_1-sparse	5.91 (30.63)	95.10 (4.88)	66.15 (2.44)	13.96 (50.61)	22.14
SalUn	33.43 (3.11)	97.61 (2.37)	61.21 (2.50)	56.27 (8.30)	4.07
SalUn-soft	32.25 (4.29)	91.01 (8.97)	58.65 (5.06)	33.60 (30.97)	12.32
GDRGMA	19.59 (16.95)	97.91 (2.07)	61.91 (1.80)	45.10 (19.47)	10.07
EUPMU	**35.18 (1.36)**	97.62 (2.36)	60.51 (3.20)	56.10 (8.47)	**3.85**
EUPMU-fast	30.18 (6.36)	97.12 (2.86)	60.81 (2.90)	49.37 (15.20)	6.83

Table 14: Results of Random Data Forgetting(30%) for various methods of unlearning Resnet 18 for Tiny-Imagenet classification. The results are the mean value over 10 independent trials. The best performance is highlighted in **bold**.

Methods	UA	RA	TA	MIA	Avg. Gap
Retrain	39.00	99.98	60.81	67.30	0.00
FT	9.75 (29.25)	**99.05 (0.93)**	64.41 (3.60)	25.65 (41.65)	18.86
RL	13.11 (25.89)	90.32 (9.66)	56.63 (4.18)	33.33 (33.97)	18.43
GA	5.14 (33.86)	95.08 (4.90)	66.01 (5.20)	14.38 (52.92)	24.22
IU	6.96 (32.04)	93.27 (6.71)	63.75 (2.94)	13.90 (53.40)	23.77
BE	10.84 (28.16)	89.12 (10.86)	**59.79 (1.02)**	18.82 (48.48)	22.13
BS	8.85 (30.15)	91.06 (8.92)	62.84 (2.03)	17.74 (49.56)	22.66
ℓ_1-sparse	5.15 (33.85)	97.31 (2.67)	65.91 (5.10)	13.61 (53.69)	23.83
SalUn	33.60 (5.40)	96.05 (3.93)	54.57 (6.24)	46.77 (20.53)	9.03
SalUn-soft	33.99 (5.01)	87.75 (12.23)	52.77 (8.04)	37.13 (30.17)	13.86
GDRGMA	22.52 (16.48)	96.00 (3.98)	55.27 (5.54)	38.96 (28.34)	13.59
EUPMU	**40.50 (1.50)**	94.05 (5.93)	50.71 (10.10)	**50.61 (16.69)**	**8.55**
EUPMU-fast	33.92 (5.08)	89.48 (10.50)	53.21 (7.60)	46.23 (21.07)	11.06

infringing or non-compliant content. By optimizing the balance between knowledge retention and targeted erasure, our methodology directly tackles the dual imperatives of model governance and regulatory compliance. The technical focus on improving governance capabilities inherently minimizes adverse societal impacts, as the proposed approach does not introduce systemic biases or operational disruptions. This dual focus not only broadens the practical applicability of machine unlearning across industries but also establishes a framework for ethically constrained AI development, aligning with regulatory demands for content accountability without compromising model utility.

Table 15: Results of Random Data Forgetting(50%) for various methods of unlearning Resnet 18 for Tiny-Imagenet classification. The results are the mean value over 10 independent trials. The best performance is highlighted in **bold**.

Methods	UA	RA	TA	MIA	Avg. Gap
Retrain	43.15	99.99	56.29	71.15	0.00
FT	7.13 (36.02)	**99.32 (0.67)**	65.27 (8.98)	18.09 (53.06)	24.68
RL	24.30 (18.85)	85.00 (14.99)	48.47 (7.82)	25.75 (45.40)	21.77
GA	4.63 (38.52)	95.35 (4.64)	66.29 (10.00)	12.96 (58.19)	27.84
IU	18.00 (25.15)	83.21 (16.78)	**56.41 (0.12)**	20.57 (50.58)	23.16
BE	7.56 (35.59)	92.47 (7.52)	62.77 (6.48)	16.62 (54.53)	26.03
BS	8.87 (34.28)	90.68 (9.31)	59.03 (2.74)	20.21 (50.94)	24.32
ℓ_1-sparse	4.44 (38.71)	95.76 (4.23)	66.39 (10.10)	12.76 (58.39)	27.86
SalUn	**44.84 (1.69)**	94.29 (5.70)	45.83 (10.46)	**54.73 (16.42)**	8.57
SalUn-soft	33.56 (9.59)	88.25 (11.74)	48.15 (8.14)	39.76 (31.39)	15.21
GDRGMA	28.73 (14.42)	91.16 (8.83)	47.73 (8.56)	36.28 (34.87)	16.67
EUPMU	31.97 (11.18)	98.50 (1.49)	52.71 (3.58)	53.18 (17.97)	**8.55**
EUPMU-fast	33.60 (9.55)	88.59 (11.40)	49.71 (6.58)	39.86 (31.29)	14.71

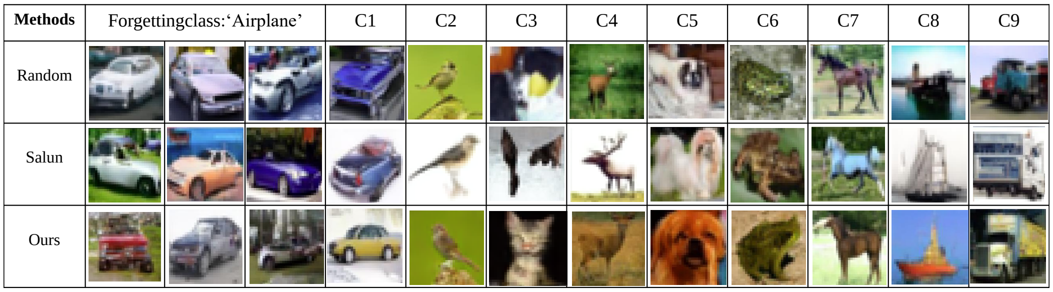

Figure 7: Image generations of unlearning for DDPM on CIFAR-10. The forgetting class is given by 'airplane', and 'C' refers to the non-forgetting class name, e.g., 'car' (C1).

NeurIPS Paper Checklist

1. **Claims**

   Question: Do the main claims made in the abstract and introduction accurately reflect the paper's contributions and scope?

   Answer: [Yes]

   Justification: The abstract and introduction in this paper accurately reflect the paper's contributions and scope.

   Guidelines:

   - The answer NA means that the abstract and introduction do not include the claims made in the paper.
   - The abstract and/or introduction should clearly state the claims made, including the contributions made in the paper and important assumptions and limitations. A No or NA answer to this question will not be perceived well by the reviewers.
   - The claims made should match theoretical and experimental results, and reflect how much the results can be expected to generalize to other settings.
   - It is fine to include aspirational goals as motivation as long as it is clear that these goals are not attained by the paper.

2. **Limitations**

   Question: Does the paper discuss the limitations of the work performed by the authors?

   Answer: [Yes]

   Justification: We provide the limitation discussion in Appendix F.

   Guidelines:

   - The answer NA means that the paper has no limitation while the answer No means that the paper has limitations, but those are not discussed in the paper.
   - The authors are encouraged to create a separate "Limitations" section in their paper.
   - The paper should point out any strong assumptions and how robust the results are to violations of these assumptions (e.g., independence assumptions, noiseless settings, model well-specification, asymptotic approximations only holding locally). The authors should reflect on how these assumptions might be violated in practice and what the implications would be.
   - The authors should reflect on the scope of the claims made, e.g., if the approach was only tested on a few datasets or with a few runs. In general, empirical results often depend on implicit assumptions, which should be articulated.
   - The authors should reflect on the factors that influence the performance of the approach. For example, a facial recognition algorithm may perform poorly when image resolution is low or images are taken in low lighting. Or a speech-to-text system might not be used reliably to provide closed captions for online lectures because it fails to handle technical jargon.
   - The authors should discuss the computational efficiency of the proposed algorithms and how they scale with dataset size.
   - If applicable, the authors should discuss possible limitations of their approach to address problems of privacy and fairness.
   - While the authors might fear that complete honesty about limitations might be used by reviewers as grounds for rejection, a worse outcome might be that reviewers discover limitations that aren't acknowledged in the paper. The authors should use their best judgment and recognize that individual actions in favor of transparency play an important role in developing norms that preserve the integrity of the community. Reviewers will be specifically instructed to not penalize honesty concerning limitations.

3. **Theory assumptions and proofs**

   Question: For each theoretical result, does the paper provide the full set of assumptions and a complete (and correct) proof?

   Answer: [Yes]

Justification: We provide the full set of assumptions and a complete (and correct) proof in Appendix C.

Guidelines:

- The answer NA means that the paper does not include theoretical results.
- All the theorems, formulas, and proofs in the paper should be numbered and cross-referenced.
- All assumptions should be clearly stated or referenced in the statement of any theorems.
- The proofs can either appear in the main paper or the supplemental material, but if they appear in the supplemental material, the authors are encouraged to provide a short proof sketch to provide intuition.
- Inversely, any informal proof provided in the core of the paper should be complemented by formal proofs provided in appendix or supplemental material.
- Theorems and Lemmas that the proof relies upon should be properly referenced.

4. **Experimental result reproducibility**

   Question: Does the paper fully disclose all the information needed to reproduce the main experimental results of the paper to the extent that it affects the main claims and/or conclusions of the paper (regardless of whether the code and data are provided or not)?

   Answer: [Yes]

   Justification: We provide the experimental information in Section 4.1.

   Guidelines:

   - The answer NA means that the paper does not include experiments.
   - If the paper includes experiments, a No answer to this question will not be perceived well by the reviewers: Making the paper reproducible is important, regardless of whether the code and data are provided or not.
   - If the contribution is a dataset and/or model, the authors should describe the steps taken to make their results reproducible or verifiable.
   - Depending on the contribution, reproducibility can be accomplished in various ways. For example, if the contribution is a novel architecture, describing the architecture fully might suffice, or if the contribution is a specific model and empirical evaluation, it may be necesssary to either make it possible for others to replicate the model with the same dataset, or provide access to the model. In general. releasing code and data is often one good way to accomplish this, but reproducibility can also be provided via detailed instructions for how to replicate the results, access to a hosted model (e.g., in the case of a large language model), releasing of a model checkpoint, or other means that are appropriate to the research performed.
   - While NeurIPS does not require releasing code, the conference does require all submissions to provide some reasonable avenue for reproducibility, which may depend on the nature of the contribution. For example
     (a) If the contribution is primarily a new algorithm, the paper should make it clear how to reproduce that algorithm.
     (b) If the contribution is primarily a new model architecture, the paper should describe the architecture clearly and fully.
     (c) If the contribution is a new model (e.g., a large language model), then there should either be a way to access this model for reproducing the results or a way to reproduce the model (e.g., with an open-source dataset or instructions for how to construct the dataset).
     (d) We recognize that reproducibility may be tricky in some cases, in which case authors are welcome to describe the particular way they provide for reproducibility. In the case of closed-source models, it may be that access to the model is limited in some way (e.g., to registered users), but it should be possible for other researchers to have some path to reproducing or verifying the results.

5. **Open access to data and code**

   Question: Does the paper provide open access to the data and code, with sufficient instructions to faithfully reproduce the main experimental results, as described in supplemental material?

Answer: [Yes]

Justification: We provide our code in the supplementary material.

Guidelines:

- The answer NA means that paper does not include experiments requiring code.
- Please see the NeurIPS code and data submission guidelines (https://nips.cc/public/guides/CodeSubmissionPolicy) for more details.
- While we encourage the release of code and data, we understand that this might not be possible, so "No" is an acceptable answer. Papers cannot be rejected simply for not including code, unless this is central to the contribution (e.g., for a new open-source benchmark).
- The instructions should contain the exact command and environment needed to run to reproduce the results. See the NeurIPS code and data submission guidelines (https://nips.cc/public/guides/CodeSubmissionPolicy) for more details.
- The authors should provide instructions on data access and preparation, including how to access the raw data, preprocessed data, intermediate data, and generated data, etc.
- The authors should provide scripts to reproduce all experimental results for the new proposed method and baselines. If only a subset of experiments are reproducible, they should state which ones are omitted from the script and why.
- At submission time, to preserve anonymity, the authors should release anonymized versions (if applicable).
- Providing as much information as possible in supplemental material (appended to the paper) is recommended, but including URLs to data and code is permitted.

6. **Experimental setting/details**

   Question: Does the paper specify all the training and test details (e.g., data splits, hyperparameters, how they were chosen, type of optimizer, etc.) necessary to understand the results?

   Answer: [Yes]

   Justification: We provide the experimental details in Appendix D.

   Guidelines:

   - The answer NA means that the paper does not include experiments.
   - The experimental setting should be presented in the core of the paper to a level of detail that is necessary to appreciate the results and make sense of them.
   - The full details can be provided either with the code, in appendix, or as supplemental material.

7. **Experiment statistical significance**

   Question: Does the paper report error bars suitably and correctly defined or other appropriate information about the statistical significance of the experiments?

   Answer: [No]

   Justification: Our experiments are averaged from multiple experiments, and the std is very small, so there is no need to report the error bar.

   - The answer NA means that the paper does not include experiments.
   - The authors should answer "Yes" if the results are accompanied by error bars, confidence intervals, or statistical significance tests, at least for the experiments that support the main claims of the paper.
   - The factors of variability that the error bars are capturing should be clearly stated (for example, train/test split, initialization, random drawing of some parameter, or overall run with given experimental conditions).
   - The method for calculating the error bars should be explained (closed form formula, call to a library function, bootstrap, etc.)
   - The assumptions made should be given (e.g., Normally distributed errors).
   - It should be clear whether the error bar is the standard deviation or the standard error of the mean.

- It is OK to report 1-sigma error bars, but one should state it. The authors should preferably report a 2-sigma error bar than state that they have a 96% CI, if the hypothesis of Normality of errors is not verified.
- For asymmetric distributions, the authors should be careful not to show in tables or figures symmetric error bars that would yield results that are out of range (e.g. negative error rates).
- If error bars are reported in tables or plots, The authors should explain in the text how they were calculated and reference the corresponding figures or tables in the text.

8. **Experiments compute resources**

   Question: For each experiment, does the paper provide sufficient information on the computer resources (type of compute workers, memory, time of execution) needed to reproduce the experiments?

   Answer: [Yes]

   Justification: We note that all experiments are carried out on two A100 GPUs in Section 4.1.

   Guidelines:

   - The answer NA means that the paper does not include experiments.
   - The paper should indicate the type of compute workers CPU or GPU, internal cluster, or cloud provider, including relevant memory and storage.
   - The paper should provide the amount of compute required for each of the individual experimental runs as well as estimate the total compute.
   - The paper should disclose whether the full research project required more compute than the experiments reported in the paper (e.g., preliminary or failed experiments that didn't make it into the paper).

9. **Code of ethics**

   Question: Does the research conducted in the paper conform, in every respect, with the NeurIPS Code of Ethics `https://neurips.cc/public/EthicsGuidelines`?

   Answer: [Yes]

   Justification: This paper focuses on theoretical results and does not involve ethical issues.

   Guidelines:

   - The answer NA means that the authors have not reviewed the NeurIPS Code of Ethics.
   - If the authors answer No, they should explain the special circumstances that require a deviation from the Code of Ethics.
   - The authors should make sure to preserve anonymity (e.g., if there is a special consideration due to laws or regulations in their jurisdiction).

10. **Broader impacts**

    Question: Does the paper discuss both potential positive societal impacts and negative societal impacts of the work performed?

    Answer: [Yes]

    Justification: We discuss both potential positive societal impacts and negative societal impacts in Appendix G.

    Guidelines:

    - The answer NA means that there is no societal impact of the work performed.
    - If the authors answer NA or No, they should explain why their work has no societal impact or why the paper does not address societal impact.
    - Examples of negative societal impacts include potential malicious or unintended uses (e.g., disinformation, generating fake profiles, surveillance), fairness considerations (e.g., deployment of technologies that could make decisions that unfairly impact specific groups), privacy considerations, and security considerations.

- The conference expects that many papers will be foundational research and not tied to particular applications, let alone deployments. However, if there is a direct path to any negative applications, the authors should point it out. For example, it is legitimate to point out that an improvement in the quality of generative models could be used to generate deepfakes for disinformation. On the other hand, it is not needed to point out that a generic algorithm for optimizing neural networks could enable people to train models that generate Deepfakes faster.
- The authors should consider possible harms that could arise when the technology is being used as intended and functioning correctly, harms that could arise when the technology is being used as intended but gives incorrect results, and harms following from (intentional or unintentional) misuse of the technology.
- If there are negative societal impacts, the authors could also discuss possible mitigation strategies (e.g., gated release of models, providing defenses in addition to attacks, mechanisms for monitoring misuse, mechanisms to monitor how a system learns from feedback over time, improving the efficiency and accessibility of ML).

11. **Safeguards**

    Question: Does the paper describe safeguards that have been put in place for responsible release of data or models that have a high risk for misuse (e.g., pretrained language models, image generators, or scraped datasets)?

    Answer: [NA]

    Justification: This paper poses no such risks.

    Guidelines:

    - The answer NA means that the paper poses no such risks.
    - Released models that have a high risk for misuse or dual-use should be released with necessary safeguards to allow for controlled use of the model, for example by requiring that users adhere to usage guidelines or restrictions to access the model or implementing safety filters.
    - Datasets that have been scraped from the Internet could pose safety risks. The authors should describe how they avoided releasing unsafe images.
    - We recognize that providing effective safeguards is challenging, and many papers do not require this, but we encourage authors to take this into account and make a best faith effort.

12. **Licenses for existing assets**

    Question: Are the creators or original owners of assets (e.g., code, data, models), used in the paper, properly credited and are the license and terms of use explicitly mentioned and properly respected?

    Answer: [NA]

    Justification: This paper does not use existing assets.

    Guidelines:

    - The answer NA means that the paper does not use existing assets.
    - The authors should cite the original paper that produced the code package or dataset.
    - The authors should state which version of the asset is used and, if possible, include a URL.
    - The name of the license (e.g., CC-BY 4.0) should be included for each asset.
    - For scraped data from a particular source (e.g., website), the copyright and terms of service of that source should be provided.
    - If assets are released, the license, copyright information, and terms of use in the package should be provided. For popular datasets, `paperswithcode.com/datasets` has curated licenses for some datasets. Their licensing guide can help determine the license of a dataset.
    - For existing datasets that are re-packaged, both the original license and the license of the derived asset (if it has changed) should be provided.

- If this information is not available online, the authors are encouraged to reach out to the asset's creators.

13. **New assets**

    Question: Are new assets introduced in the paper well documented and is the documentation provided alongside the assets?

    Answer: [NA]

    Justification: This paper does not release new assets.

    Guidelines:

    - The answer NA means that the paper does not release new assets.
    - Researchers should communicate the details of the dataset/code/model as part of their submissions via structured templates. This includes details about training, license, limitations, etc.
    - The paper should discuss whether and how consent was obtained from people whose asset is used.
    - At submission time, remember to anonymize your assets (if applicable). You can either create an anonymized URL or include an anonymized zip file.

14. **Crowdsourcing and research with human subjects**

    Question: For crowdsourcing experiments and research with human subjects, does the paper include the full text of instructions given to participants and screenshots, if applicable, as well as details about compensation (if any)?

    Answer: [NA]

    Justification: This paper does not involve crowdsourcing nor research with human subjects.

    Guidelines:

    - The answer NA means that the paper does not involve crowdsourcing nor research with human subjects.
    - Including this information in the supplemental material is fine, but if the main contribution of the paper involves human subjects, then as much detail as possible should be included in the main paper.
    - According to the NeurIPS Code of Ethics, workers involved in data collection, curation, or other labor should be paid at least the minimum wage in the country of the data collector.

15. **Institutional review board (IRB) approvals or equivalent for research with human subjects**

    Question: Does the paper describe potential risks incurred by study participants, whether such risks were disclosed to the subjects, and whether Institutional Review Board (IRB) approvals (or an equivalent approval/review based on the requirements of your country or institution) were obtained?

    Answer: [NA]

    Justification: This paper does not involve crowdsourcing nor research with human subjects.

    Guidelines:

    - The answer NA means that the paper does not involve crowdsourcing nor research with human subjects.
    - Depending on the country in which research is conducted, IRB approval (or equivalent) may be required for any human subjects research. If you obtained IRB approval, you should clearly state this in the paper.
    - We recognize that the procedures for this may vary significantly between institutions and locations, and we expect authors to adhere to the NeurIPS Code of Ethics and the guidelines for their institution.
    - For initial submissions, do not include any information that would break anonymity (if applicable), such as the institution conducting the review.

16. **Declaration of LLM usage**

Question: Does the paper describe the usage of LLMs if it is an important, original, or non-standard component of the core methods in this research? Note that if the LLM is used only for writing, editing, or formatting purposes and does not impact the core methodology, scientific rigorousness, or originality of the research, declaration is not required.

Answer: [NA]

Justification: This research does not involve LLMs as any important, original, or non-standard components.

Guidelines:

- The answer NA means that the core method development in this research does not involve LLMs as any important, original, or non-standard components.
- Please refer to our LLM policy (`https://neurips.cc/Conferences/2025/LLM`) for what should or should not be described.